

Review

# Cross-Linked Polymeric Gels and Nanocomposites: New Materials and Phenomena Enabling Technological Applications

Cesar A. Barbero <sup>\*</sup>, María V. Martínez, Diego F. Acevedo , María A. Molina  and Claudia R. Rivarola

Research Institute for Energy Technologies and Advanced Materials (ITEMA), National University of Río Cuarto (UNRC)-National Council of Scientific and Technical Research (CONICET), Río Cuarto 5800, Argentina  
\* Correspondence: cesarbarbero@gmail.com

**Abstract:** Cross-linked gels are synthesized by homo- and copolymerization of functionalized acrylamides. The gels swell in aqueous solution, and some of them (e.g., poly(N-isopropylacrylamide (PNIPAM)) also in organic solvents of low polarity (e.g., dichloromethane), making the gels amphiphilic materials. Nanocomposites can be made by dispersing nanoparticles (metallic, graphene, nanotubes, and conducting polymers) inside the gels. Additionally, true semi-interpenetrated networks of polyaniline (PANI) inside PNIPAM gels can be prepared by swelling the gel in true solutions of PANI in NMP. PNIPAM-based nanocomposites show a lower critical solution temperature (LCST) transition of the gel matrix, which can be reached by thermal heating or absorption of electromagnetic radiation (light, microwaves, radiofrequency) in the conductive nanomaterials. The characteristic properties (swelling degree and rate, LCST, solute partition, mass transport, hydrophilicity, biocompatibility) can be tuned by changing the functional groups in the copolymers and/or the other components in the nanocomposite. Mass transport and mechanical properties can be adjusted by forming materials with macro- (nanoporous and macroporous), micro- (microgels, thin films, Pickering emulsions), or nano- (nanogels, stabilized nanoparticles) sized features. The material properties are used to produce technological applications: sensors, actuators, controlled release, biological cell scaffolds and surfaces, antimicrobial, carriers of bioactive substances, and matrixes to immobilize enzymes and yeast cells.

**Keywords:** conducting polymers; LCST; photothermomechanical; sensors; drug release; actuators



**Citation:** Barbero, C.A.; Martínez, M.V.; Acevedo, D.F.; Molina, M.A.; Rivarola, C.R. Cross-Linked Polymeric Gels and Nanocomposites: New Materials and Phenomena Enabling Technological Applications. *Macromol* **2022**, *2*, 440–475. <https://doi.org/10.3390/macromol2030028>

Academic Editors: Paul Joseph, Svetlana Tretsiakova-McNally and Malavika Arun

Received: 4 July 2022

Accepted: 7 August 2022

Published: 2 September 2022

**Publisher's Note:** MDPI stays neutral with regard to jurisdictional claims in published maps and institutional affiliations.



**Copyright:** © 2022 by the authors. Licensee MDPI, Basel, Switzerland. This article is an open access article distributed under the terms and conditions of the Creative Commons Attribution (CC BY) license (<https://creativecommons.org/licenses/by/4.0/>).

## 1. Introduction

Acrylamides and related polymers (e.g., acrylic acid (AA)) can polymerize (with bifunctional monomers as cross-linkers) to form lightly cross-linked tridimensional networks. These materials swell strongly in water and belong to the hydrogel family. As such, they are widely used in both industry [1] and academia [2] due to their versatility, easy homo-/copolymerization, and availability of different functional monomers [3]. The main properties of interest are large swelling in water [4], good biocompatibility [5], and optical transparency [6]. Besides that, some of them show volume changes driven by temperature [7], pH [8], or ionic strength [9]. Polyacrylamide is hydrophilic and forms hydrogen bonds with water molecules due to the amide groups of the polymeric chain. Moreover, by copolymerization with acrylamides bearing functional groups (e.g.,  $-\text{SO}_3^-$  within AMPS or  $-\text{NR}_4^+$  within AMPTAC), fixed charges could be attached to the chains, thus making the gels more hydrophilic for two reasons: (i) water has ion-dipole interactions; (ii) the counterions of the fixed charges (e.g.,  $\text{Na}^+$ ) dissolved in the inner solution increase the osmotic pressure inside the gel. The later process leads to a large swelling of gels in water (superabsorbency) since the flexible network tends to imbibe water to decrease the osmotic pressure inside the gel. On the other hand, copolymerization with acrylamides bearing alkyl chains (e.g., isopropyl in NIPAM) makes the gel more hydrophobic, inducing swelling in less polar solvents. The polymerization is usually carried out

in water, and the materials can be conformed as macroscopic shapes, thin films, micro-, and nanoparticles. The networks are usually nanoporous but could be also fabricated as macroporous gels (e.g., by cryogelation). The gels can be used as matrixes of nanocomposites and semi-interpenetrated networks. Additionally, linear polyacrylamides could be used as smart molecular materials (by block copolymerization with conducting polymers), nanoparticle stabilizers, and binders of nanomaterials. They can be applied in diverse fields: biomedical research; electrochemistry; analytical chemistry and in technologies such as electromechanical sensor/actuators; biofuel synthesis; remediation; and so on. The final properties of the material (e.g., swelling degree) have to be tuned to the specific application. This can be performed by including functional groups (e.g., by copolymerization) and/or by combining with other materials, creating blends or composites. On the other hand, the physical form/size of the material could be also changed to produce specific properties (e.g., fast swelling rate). In our research group, we have studied polyacrylamide gels and their composites with other materials (conducting polymers, metals, graphene, biological entities) for different applications. Besides, we have explored several architectures: nanoporous and macroporous gels, thin films, micro-, and nanoparticles [10–49]. Along those works, we observed that studies in the field involves some implicit or explicit paradigms:

- (i) Gels can be formed by homopolymerization or copolymerization of any acrylamide, and the relative reactivity of the comonomers is always the same, whatever is the functional group attached to the amide.
- (ii) Any acrylamide can be polymerized (together with a cross-linker) into a solid hydrogel using the same initiator (e.g., APS/TEMED).
- (iii) The incorporation of a linear conductive polymer inside the gel by in situ polymerization produces a semi-interpenetrated network.
- (iv) The swelling of the hydrogel intake water and ions dissolved in it, in the same concentration as in solution. Conversely, if the gel collapses (e.g., by reaching LCST), water is expelled and the ions are loaded inside.
- (v) If the gel contains fixed charged groups, the mobile counterions are taken into the network and the co-ions are excluded (Donnan exclusion).
- (vi) Macroporous hydrogels are mechanically weaker than their nanoporous counterparts due to the lower percentage of solid material.
- (vii) Gels, as solids, have defined interfaces with the solution.
- (viii) Hydrogels swell in water and similar solvents (e.g., alcohols) but not in low-polarity solvents (e.g., chloroform).
- (ix) Loading of substances to be released has to be performed from aqueous solution, even for molecules almost insoluble in water.
- (x) It is not possible to trap biological entities (enzymes, cells) by in situ radical polymerization/gelation since radicals themselves and/or acrylamides themselves are deleterious to those entities.

We observed results that sometimes confirm but mostly challenge those established paradigms, and the subject will be discussed in the text.

First, new fabrication methods used to produce different gel structures will be presented. Then, the improved strategies used to tune the material properties towards technological applications will be discussed. Finally, different prototype systems where those novel properties are applied will be shown.

## 2. Summary of Experimental Procedures

Monomers (AAM, NIPAM, AMPS, AMPTAC, BIS, AA, HMA, NAT, ANI, Py) and polymers (PS, HPC, PMMA, PVA) were provided by Sigma-Aldrich (St. Louis, MO, USA) and used as received. Reactants (APS, TEMED, sodium oxalate, Bphen Phen) and auxiliary compounds (Rubipy, Sodium phosphate, HCl, AgNO<sub>3</sub>, SPAN 80, methacryloxypropyltrimethoxysilane, 4-ATF, MTT) were provided by Merck and used as received. Multiwall carbon nanotubes were provided by Nanoshel. GO was kindly provided by G.M. Morales

(UNRC). Solvents were provided by Sintorgan (AR) and were of analytical quality. Further details are described in the references.

SEM measurements were performed in a EVO MA10 (Carl Zeiss, Jena, Germany) microscope. Optical microscopy was performed in a Arcano S300 (Beijing, China) microscope. DLS measurements were performed in a Malvern 4700 (Madison, WI, USA) equipment. Mechanical measurements were performed with a homemade system and/or a NETZCH 242 E DMA (Selb, Germany). Differential scanning calorimetry measurements were made in a NETZCH (Selb, Germany) 204 F1 device. Weights were measured with an analytical balance (Sartorius, Bohemia, NY, USA) with 0.01 mg resolution.

#### **Fabrication of materials**

Polyacrylamide gels can be produced in different forms (nanoporous, macroporous) and sizes (bulk, thin films, micro-/nanoparticles). The chemical composition could be adjusted by copolymerization of a simple monomer (e.g., AAm) and a functional monomer (e.g., AMPS). The gels can act as matrixes of nanocomposites containing nanoparticles (metallic, graphene, carbon nanotubes, conducting polymers). These networks can be also used to immobilize biological entities, such as enzyme or yeast cells. They can also contain linear polymers interpenetrated into the 3D matrix, giving semi-interpenetrated networks. Below, the typical methods we used to produce those materials are discussed.

### *2.1. Macroscopic Gels*

#### *2.1.1. Nanoporous*

Nanoporous polyacrylamide gels were synthesized via free-radical homopolymerization of one monomer (e.g., PNIPAM [7]) using a cross-linking agent (e.g., BIS). APS and TEMED were used as the redox radical initiator. Incorporation of functional groups to the chains can be made by copolymerization of a simple acrylamide (e.g., AAm) with a functionalized acrylamide (e.g., AMPS). The relative amount (e.g., 2% mol/mol) of a cross-linker was calculated, taking the number of moles of all vinylic monomers present as 100%.

In a typical procedure, BIS was dissolved in aqueous solution of vinyl monomers (0.5 M in total), and the solution was purged by bubbling N<sub>2</sub> gas to eliminate O<sub>2</sub> (polymerization inhibitor). Then, the polymerization initiator system (APS (0.001 g/mL)/TEMED (10 µL/mL)) was added. The polymerization was carried out in a sealed tube at room temperature (20 °C) for 3 h to achieve the gelation. Then, to remove unreacted chemicals, the hydrogels were immersed in distilled water (renewed several times) at room temperature for 48 h. The gel cylinder was cut in small discs of ~2 mm thickness. The discs were dried in an oven at 50 °C until constant weight (ca. 24 h).

#### *2.1.2. Macroporous*

##### *Directional Cryogelation*

Macroporous hydrogels were produced by free radical polymerization at −18 °C using the same prepolymeric solution used for nanoporous gels (Section 2.1.1) but without purging with nitrogen. In that way, the dissolved oxygen delayed the onset of polymerization until freezing occurred. For the same purpose, the initiators were added at 0 °C. The solution was then transferred to a plastic syringe and sealed with wax. Immediately, the syringe was placed inside a block of Styrofoam, where it fit tightly, leaving the syringe ends open to the exterior. In that way, the cooling occurred directionally from both extremes, while the walls of the syringe were isolated from the freezer. The whole setup was placed in a freezer (T = −18 °C) and kept undisturbed for 24 h for the polymerization to take place. In this way, long narrow ice crystals were grown. Otherwise, the crystals grew from the wall to the center, producing a gel, which was quite easy to fall apart when taken out of the syringe. Then, the content of the syringe was extracted and thawed at room temperature (2 h). The wet hydrogel was thoroughly washed with running deionized water to remove unreacted chemicals. As shown below (Section 2.2), the elasticity modulus was low in the direction perpendicular to the pores.

## Gas Templating

Polymerization is carried out following the same procedure described before (Section 2.1.1) with the addition of up to 10% (%molar to the monomer) oxalate ions to the pregel solution. The gas (CO<sub>2</sub>) was formed in situ by reaction of APS with the oxalate ions. Since APS will be consumed by this reaction and it will not be available for radical initiation, an extra equimolar amount of APS to oxalate is also added to the polymerization solution.

## 2.2. Thin Films

The hydrogel chains were grafted to a glass slide by pretreating the glass surface with methacryloxypropyltrimethoxysilane to form a monolayer of covalently linked vinyl groups. Then, a thin film of pregel solution was spread onto the glass. The glass slide was placed into a sealed plastic chamber, which was flushed with nitrogen to avoid the presence of oxygen. After 3 h, the slide was removed, washed with distilled water, and dried in a vacuum oven.

## 2.3. Nanoparticles

### 2.3.1. Nanogels

Polyacrylamide nanogels were obtained by precipitation copolymerization. The molar composition of the nanogels was: neutral monomer (e.g., NIPAM): 96.5%, BIS 1.5%, and charged monomer (e.g., AMPS): 2%, using a total monomer concentration of 120 mM in water. The charged monomer is required to stabilize the colloidal solution of the nanogels. The neutral monomer and BIS were first mixed in a final volume of 10 mL, deoxygenated with gaseous nitrogen, and heated to 70 °C, while stirring for 1 h. Subsequently, the charged monomer and 2 mM of APS in 1 mL of water were added. The temperature, stirring, and degassing with nitrogen were maintained for 4 h. The nanogels were washed by cycles of centrifugation (14,000 rpm), followed by redispersion in distilled water. The nanogels could not be dried conventionally because they could irreversibly aggregate, but the dispersion could be lyophilized to produce dry nanoparticles.

### 2.3.2. Smart Nanoparticles Stabilized by Polyacrylamides

PANI nanoparticles were produced by precipitation polymerization using hydrophilic polyacrylamides as stabilizers. A 0.2 M solution of aniline hydrochloride was oxidized with 0.25 M APS in the presence of 1% (*w/w*) of the chosen polyacrylamide as stabilizer (e.g., PNIPAM). The polymerization of aniline was started at 20 °C by adding an aqueous solution of APS. The mixture was briefly stirred and left undisturbed for 30 min to polymerize. The nanoparticles were washed by centrifugation/redispersion (in pure water) cycles.

### 2.3.3. Block Copolymers of Acrylamides and Anilines

The polymerization of an acrylamide (e.g., NIPAM) (1 M) was carried out in water with a thermally activated initiator (VA044) ( $5 \times 10^{-3}$  g/mL) at 60 °C under nitrogen bubbling during 4 h. The thiol 4-ATF ( $3 \times 10^{-5}$  M) was used as a chain transfer agent, producing a polyacrylamide terminated with aniline groups. The polymer was precipitated in methanol, obtaining the PNIPAM-S-ANI as a white solid. The oxidative polymerization of anilines (e.g., ANI) was carried out using 0.1 M monomer (e.g., ANI) in 1 M HCl at 0 °C. Then, APS (equimolar to the monomer) was added as an oxidant agent to produce the polymer. The conducting polymer block grew from the terminal ANI group at the modified polyacrylamide, producing a block copolymer (poly(acrylamides-*b*-anilines)). Finally, the product was precipitated with methanol, washed, and dried [39].

## 2.4. Microparticles

Hydrogel microspheres were obtained by inverse emulsion polymerization. The pregel solution was prepared by dissolving NIPAM (0.5 M), AMPS (feed ratio: 0.98:0.2), and BIS as a cross-linker (2% moles) in water. The polymerization solution was dispersed in cyclohexane, containing a surfactant (SPAN 80), with strong stirring to form an inverse

emulsion. The emulsion was agitated at 50 °C for 30 min, and the initiator was added (APS, 4 mM). After that, the emulsion was agitated for 5 h at 50 °C. The hydrogels microspheres were separated by centrifugation, washed with distilled water, and dried.

## 2.5. Nanocomposites

### 2.5.1. With Metallic Nanoparticles

A novel procedure to synthesize silver nanoparticles inside the hydrogels was developed [29]. Dry hydrogel discs were submerged in 3 mL of AgNO<sub>3</sub> (0.01 M) solution for 24 h to ensure that the absorption of Ag<sup>+</sup> ions reached a partition equilibrium state and maximum swelling capacity. The swollen discs were then illuminated with UV light (broadband fluorescent lamp, 20 W) situated at less than 5 cm from the sample for 8 h. This time is required to obtain a large enough concentration of Ag-NPs inside the hydrogel. The colorless gel becomes yellow-light brown due to the plasmon electronic absorption of Ag nanoparticles.

### 2.5.2. With Conductive Polymer Nanoparticles

#### Filling the Pores by In Situ Polymerization/Precipitation

Small pieces (with at least one dimension smaller than 2 mm to allow fast mass transport) of dry hydrogels were immersed into the polymerization solution, which was prepared by dissolving 0.1 M of the conducting polymer (CP) monomer (anilines or pyrrole) in 0.1 M HCl/water. The simultaneous swelling and loading of the monomer was facilitated by stirring during 12 h. Then, an equimolar (to the CP monomer) amount of APS was added as oxidant to produce the CP inside the gel. This order of addition of reactants is required; otherwise, nonhomogeneous or degraded materials are obtained. It should be borne in mind that an excess of CP monomer is irrelevant, while an excess of APS causes polymer degradation [50]. While in solution, this effect can be controlled by proper feed ratio and stirring inside the gel, depending on the mass transport in the solid. The polymerization was carried out at room temperature for 3 h. The nanocomposite samples were then immersed in flushing stirred distilled water (>1 L) at room temperature for at least 48 h in order to extract unreacted chemicals. The colorless hydrogel became highly colored at the end of the polymerization, indicating that the CP was loaded inside the hydrogel matrix. By visual observation of a sectioned hydrogel piece, it can be checked whether the CP was uniformly loaded inside the hydrogel [13].

#### Trapping of Preformed Nanoparticles

Nanocomposites were synthesized by free radical polymerization of acrylamides (e.g., NIPAM) at 0.5 M using BIS as a cross-linker (2% of total monomer moles) in the presence of the preformed nanoparticles. The monomer and cross-linker were dissolved in a diluted dispersion (0.1 mg/mL) of nanoparticles (e.g., PPy NP). Then, the polymerization initiator system (APS (0.01 g/mL) and TEMED (10 mL mL/1)) was added. The cross-linked hydrogel grew around the nanoparticles, trapping them in the matrix, gelling in 1–2 h [42].

### 2.5.3. Graphene

The nanocomposites were synthesized by free radical polymerization of acrylamides in cylindrical molds in the presence of GO. Acrylamides (1 M) were employed as monomer and BIS (0.310 mg/L) as a cross-linking agent. The polymerization was initiated by a redox initiator system: APS (1 µg/mL) and TEMED (1 µL/mL). The monomer and APS were first dissolved in 4 mL of PBS buffer (pH 5.8), and 20 mg of GO was added and dispersed with ultrasound. Then, TEMED was added to produce the polymerization in 24 h. Then, the nanocomposites were cut into slices, washed several times with distilled water, and dried for 48 h at room temperature under moderate vacuum. The dried samples were stored in a desiccator for later use [35].

#### 2.5.4. Carbon Nanotubes

The nanocomposites were made by synthesis of the nanoporous gels (as described in Section 2.1.1), replacing part of the water by dispersion of MWNTs (1.5 mg/mL) in water. To disperse the MWNTs in water, first, they were oxidized and cut. With this purpose, 2.5 g of multiwalled CNTs were treated with 26 mL of 3:1 (molar) solution of H<sub>2</sub>SO<sub>4</sub> and HNO<sub>3</sub> for 3 h at 80 °C with magnetic stirring. The treatments degrade/dissolve impurities, create oxygen-containing groups in the surface, and decrease the length. The treated CNTs were then washed repeatedly with deionized water until a pH of the solution was neutral. Finally, the purified CNTs were dried in a vacuum oven for 24 h at 100 °C. For stabilization of the MWNT dispersion, chitosan (75% deacetylation, MW = 100 kDa) was used. An amount of 100 mg of MWNT was dispersed in a chitosan solution (0.1 g in 100 mL of 1% acetic acid solution). The mixture was treated in an ultrasonic bath for 10 min and then stirred for 1 h. During this step, chitosan macromolecules were adsorbed on the surface of the CNTs, thereby stabilizing the MWNT dispersion [17].

#### 2.5.5. Enzymes

An amount of 0.3 mL of  $\alpha$ -amylase solution (containing 0.088 mg of  $\alpha$ -amylase) was added to 4 mL of the polymerization solution (used to produce nanoporous hydrogel; see Section 2.1.1) with or without the addition of GO [37]. It is noteworthy that amylases contain cysteine groups [51], which could act as chain transfer agents in the radical polymerization [52]. In that way, the hydrogel chains become linked to the enzyme backbone. However, no effect on the chemical activity of the enzyme due to the free radicals was observed.

#### 2.5.6. Yeast Cells

Commercial yeast (*Saccharomyces cerevisiae*) from a bioethanol industry was hydrated in PBS for 1 h prior to mixing with the pregel solution (the same used for the preparation of nanoporous gels of acrylamide; see Section 2.1.1). The yeast dispersions (containing 25–250 mg of yeast) were added to 1 L of solution. Additionally, the same mixture was used to produce macroporous gels by cryogelation without the addition of cryoprotective agents [25]. It is noteworthy that acrylamide and free radicals (produced during polymerization) are normally toxic for microorganisms, but no effect was observed in this case, allowing a simple procedure to produce the composite.

#### 2.6. Semi-Interpenetrated Networks (s-IPN)

To the best of our knowledge, the only way to produce true s-IPN of conducting polymers in gels involves swelling the gel in a true solution of the conducting polymer [33], since in situ polymerization produces a nanocomposite (see Section 2.5.2). Therefore, a solvent is required that swells the gel (e.g., PNIPAM) and, at the same time, dissolves the conducting polymer (e.g., PANI). It is known that PANI (in its emeraldine base form) dissolves in NMP [53], and NMP has also been found to swell PNIPAM [33]. To semi-interpenetrate PANI in PNIPAM gels, small discs of dry hydrogels were swelled in a true solution of PANI (base form) in NMP as a solvent at room temperature for 48 h. Then, the discs were immersed in flushing stirred distilled water (>1 L) at room temperature for at least 48 h to extract NMP. The composite was then treated with HCl solution in order to convert PANI base into a conductive form and completely extract the NMP.

#### Characterization methods

#### 2.7. Microscopy

Different microscopies could be used to characterize gels. While optical microscopy (with staining) and AFM could be made on the wet or dry state, others (SEM, TEM) usually require drying the gels. Therefore, lyophilization should be used. Otherwise, features such as macropores or crevices arise by the water meniscus forces during drying.

### 2.8. Absorption of Solvents, Equilibrium, and Kinetics

The swelling of the synthesized hydrogels in water as a function of time is usually studied through gravimetric analysis. The dry hydrogels were weighed ( $Wd$ ) and then placed in beakers with a solvent (e.g., distilled water) at a constant temperature. At different times, the wet gel was removed from the beaker, the excess solvents were removed with tissue paper, and hydrogel was weighed ( $Ww(t)$ ). The swelling percentage ( $\%Sw(t)$ ) changes with time and is calculated by Equation (1) [10–13,15,16,19,23,26,29]:

$$\%Sw(t) = \left[ \frac{Ww(t) - Wd}{Wd} \right] * 100 \quad (1)$$

The swelling percentage is a practical way to compare different gels in water. Graphics of  $\%Sw(t)$  versus time were made to analyze the swelling kinetic of hydrogel matrices. The environment of the sample should be kept at the same temperature; otherwise, the measurement of kinetics would be in error. Typical gel samples are disks of ca. 2 mm in thickness, which could take several days to reach the equilibrium value ( $\%Sw$ ). The use of Equation (1) to evaluate swelling assumes that no part of the gel dissolves in water or disintegrates. While this is usually true for covalent linked gels, it is not the case for gels made of noncovalent cross-links (e.g., PVA-based gels cross-linked by crystalline domains [53,54]). To check the assumption, the dry weight of the material is measured before and after swelling, and the mass percentage ratio calculated [53,54]. A value close to 100% makes Equation (1) valid.

In the case of different solvents, Equation (1) is not useful since solvents of larger molecular weights will show a larger value for the same amount of absorbed molecules. Therefore, Equation (2) is used:

$$AbsCap(t) = \left[ \frac{(Ww(t) - Wd)}{Wd * MW} \right] \quad (2)$$

where  $MW$  is the molecular weight (g/mol) of the solvents, and  $AbsCap(t)$  is a molal concentration of solvent inside the gel related to the number of solvent molecules absorbed per kg of gel. Therefore, it allows us to compare the absorption capacity of different solvents. In the case of solvent mixtures (e.g., ethanol/water), a mean value of  $MW$  is used, calculated with the molar fraction and the respective molecular weights.  $AbsCap(t)$  reaches a constant value ( $AbsCap$ ) after an equilibrium time.

### 2.9. Porosity

Macroporosity could be directly determined by drying the gel (by lyophilization to avoid pore collapse), weighing, and filling the pores with a solvent, which do not swell the gel (e.g., cyclohexane). The added weight (divided by the density of the solvent) gives the pore volume. The ratio with the total volume (determined from the dimensions) gives the volumetric porosity.

### 2.10. Lower Critical Solution Temperature (LCST)

Several properties of the networks change at the LCST. The volume decreases significantly (<100%), the gel becomes opaque, heat is absorbed, and solution is expelled. While all these properties can be used, visual observation of the gel is the most usual. However, DSC, which determines the heat absorbed by the sample, is the most accurate and could detect multiple transitions in a narrow temperature range [29].

### 2.11. Mechanical Properties

The elastic modulus can be directly determined by measuring the deformation upon application of a force (or pressure). However, special equipment is required since typical mechanical test machines apply large forces (>10 kN) without enough resolution. A homemade equipment was settled using a balance (res.  $10^{-3}$  N) to measure applied force,

a micrometric screw to apply force, and an electromechanical sensor (res. 1  $\mu\text{m}$ ) to measure displacement. The same system was extended to simultaneously measure resistance, using two metal covered slides as contact surfaces [16].

### 2.12. Contact Angle

Like other surfaces, the contact angle of a solvent can be measured by placing a small drop of solvent on the surface and photographing the shape of the drop from the side with a microscope. The image can be processed with a free software (ImageJ) using a special plug-in [54]. The surface should be flat at the nanometric level since it is known that surface topography has effect on the measured contact angles [55]. It is important to point out that the surface of gel pieces arises from cutting or reflects the surface of the mold. Therefore, surfaces arising from clean cuts of gels with microtomes or by gelling on polished surfaces should be used.

### 2.13. Biocompatibility/Toxicity

In biological applications, the gels do not have to release toxic substances or produce lysis/death of biological cells. Since monomers (acrylamides) are usually carcinogenic and toxic, careful washing of the gels should be performed. For biocompatibility studies, cells were cultivated during 24 h in contact with the sterilized hydrogels and using polystyrene a multiwell plate's surface as a control system. Then, an MTT assay was carried out to measure the absorbance at 540 nm due to formazan formation [56] in living cells. To evaluate toxicity/teratogenicity, pieces of hydrogel were placed in the media where frog toads were growing during 5 days. The number of dead and/or malformed individuals was compared with a control.

## 3. Results and Discussion

### 3.1. Fabrication of Different Shapes/Forms

In the first part of this section, the methods for fabricating the gels in different forms are described.

#### 3.1.1. Nanoporous Gels

Polyacrylamide gels can be easily made as macroscopic shapes. Indeed PAAm cross-linked gels are the most common materials for gel electrophoresis. Polymerization of an acrylamide monomer (e.g., AAm) together with an appropriate cross-linker (e.g., BIS) in a concentrated aqueous solution renders a solid gel, which fills the mold or copies the shape of the solution. Being soft, the bulk materials can be cut in different shapes. Since the radical polymerization produces a distribution of chain lengths with a random distribution of cross-links, the structures are a 3D network with open and connected nanopores (<100 nm). Accordingly, the gel can incorporate molecules, but even large nanoparticles (ca. 200 nm) could not be loaded in the gels and remain adsorbed on the surface [12]. More complex gels can be made by copolymerization of different acrylamides or even similar vinyl compounds, such as acids (e.g., AA) or esters (e.g., MMA). One condition is that all monomers are dissolved in the solvent; therefore, nonaqueous solvents (e.g., DMF) are used when any monomer is insoluble in water. Redox initiators (e.g., APS/TEMED) are the most commonly used because they can be performed in water at different temperatures. On the other hand, thermal initiation requires heating the mixture, and this could affect the solubility of the polymer. Massive nanoporous gels show large characteristic mass transport times (e.g., time to completely release a substance from the gel) due to the low diffusion coefficients (<math>10^{-8}</math>  $\text{cm}^2/\text{s}$ ) and absence of other mass transports (e.g., convection) present in liquids. In a diffusion-controlled process, mass transport inside solid gel slabs (with a thickness much smaller than the side), the characteristic time ( $t_c$ ) is given by Equation (3):

$$t_c \approx \frac{x^2}{2D} \quad (3)$$



where  $x$  is the thickness of the slab. The mass transport of water inside the gel also affects the time for swelling. On the one hand,  $D$  can be increased with the pore size, which can be performed by decreasing the amount of the cross-linker. However, the mechanical properties (e.g., elastic modulus) also decrease. On the other hand, lowering  $x$  decreases  $t_c$  in a quadratic fashion. This can be performed by using thin films, macroporous solids, or small particles (micro- or nanoparticles).

### 3.1.2. Macroporous Gels

As discussed above, even nanoparticles could not be loaded inside nanoporous hydrogels. However, macroscopic shapes of macroporous gels can be made if proper micrometric-sized molds, which can be removed after polymerization, are dispersed in the gel matrix. In that sense, gas ( $\text{CO}_2$ ) bubbles are produced by reaction of oxalate and APS (already present as initiator). Closed spherical gels are imprinted inside the hydrogel. The density and mechanical properties decrease, but nanoparticles cannot be loaded inside the gel because the porosity is closed. (Figure 1).

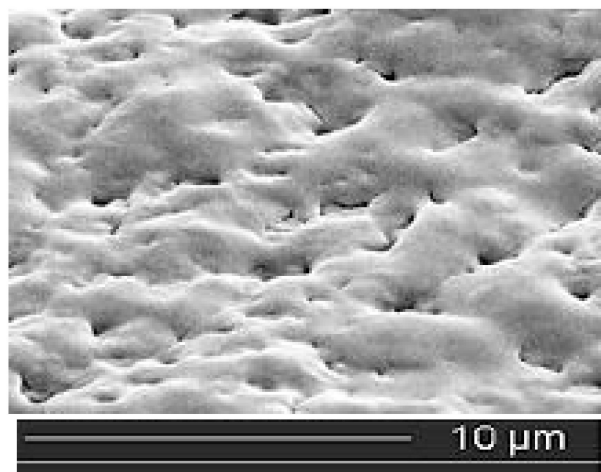


**Figure 1.** SEM micrograph of PNIPAM (cross-linked with 2% BIS) made in the presence of 5% sodium oxalate.

In another approach, oriented ice crystals (needles) of micrometric diameter can be made by directional congelation of the pregel solution using a commercial freezer ( $T = -18\text{ }^\circ\text{C}$ ). At such temperature, redox-initiated polymerization occurs in 48–72 h. Since the water is frozen, polymerization occurs in a highly concentrated monomer solution, producing shorter chains between cross-links, producing a more compact gel. After synthesis, the ice is melted or sublimated by applying vacuum (lyophilization), rendering a nanoporous gel matrix bearing oriented micrometric macropores. As it will be discussed later, the mechanical properties of the pore walls are different from those of the material made at room temperature. Interestingly, the copolymer of NIPAM with AMPS renders elongated interconnected pores, while cryogelated P(NIPAM-co-HMA) shows spherical closed cavities [20]. It seems that -OH-bearing groups, similar to sugars, act as cryoprotective agents producing small nearly spherical ice crystals. Other methods have been used to produce macroporous gels [57].

### 3.1.3. Thin Films and Submicrometric Structures

Thin films on surfaces are interesting materials for technological applications because the mass transport (including water intake during swelling) is fast (due to the shorter diffusion path lengths); they are likely to be transparent with a large ratio surface/volume. If a thin layer of pregel solution is placed on a flat surface, and the polymerization is initiated; thin films ( $<10\text{ }\mu\text{m}$ ) of cross-linked hydrogel can be formed. Besides the redox initiation, photochemical initiation could be used since light can reach the whole thickness

of the solution [10]. The substrate (e.g., glass) is previously treated with a reactant (e.g., vinylchlorosilane), which allows the formation of a monolayer of attached vinyl groups. Therefore, some chains are linked to the substrate bonding the film to it. Special care has to be taken to place the solution film in a closed chamber, which can be degassed to avoid the inhibiting effect of oxygen. Periodic submicrometric structures can be inscribed on the thin films by gel ablation using direct laser interference patterning (DLIP) [58]. For that purpose, light has to be absorbed in the film to produce photothermal ablation. Therefore, a dye is absorbed into the hydrogel. The DLIP procedure is performed in the dry state, and periodic structures (e.g., grooves) are observed by optical microscopy or AFM. Interestingly, when the film is swollen in water, the grooves disappear because neighboring ridges expand by swelling to close the gap [14]. Therefore, the topography (and related properties, such as optical diffraction, wettability, and cell adhesion) could be switched by heating/cooling. A colored material can be also made by the formation of a conducting polymer (PANI) inside the gel (nanocomposite). PANI absorbs light, heating up and allowing laser ablation (DLIP) of the gel. Moreover, the material has photothermomechanical properties (see below). Therefore, the topography could also be switched by the application of electromagnetic radiation [42].

#### 3.1.4. Nanogels and Microgels

As discussed above, micro- and nanoparticles should show fast response (small switching time) and form colloidal solutions resembling molecular systems [59]. Nanogels are synthesized by polymerization of acrylamides (and cross-linker) in dilute solution and with a larger amount of initiator. In that way, particle nuclei are formed that grow to the desired size. However, nonstabilized particles could aggregate and form massive gels. To stabilize the dispersions, charged surfactants (e.g., SDS) are added, which adsorb on the particle surface. The exposed charges are compensated by a layer of mobile counterions, and the charged double layers of different particles repel each other, inhibiting aggregation. However, the surfactants are usually not biocompatible. Therefore, charged particles are created by copolymerization with a small amount of functionalized monomers (e.g., AMPS) [60]. Relatively large nanoparticles (>200 nm, Figure 2) can be produced [61].

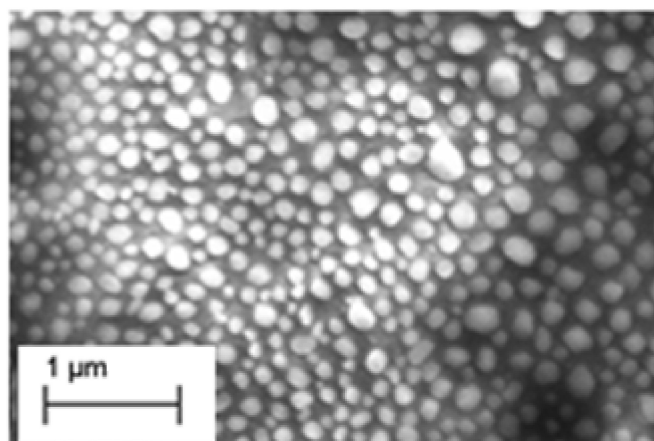


**Figure 2.** SEM image of cross-linked P(NIPAM-co-2%AMPS) nanop. articles deposited onto a glass slide. Taken in low-vacuum mode without metallization.

Small (diameter <math><25\text{--}50\ \mu\text{m}</math>) microspheres form colloidal solutions and could be applied in a similar way as in nanogel dispersion. The fabrication method involves the formation of an emulsion of aqueous polymerization solution in nonpolar media (e.g., cyclohexane) using a nonionic surfactant (e.g., SPAN 80) as an emulsion stabilizer. The solution droplets act as a mold of the nanoporous gels. One advantage is the fact that they can be separated by filtration and observed by optical microscopy. Interestingly, like other colloids of solid microparticles [62], the microparticles self-assemble on charged

surfaces by columbic interaction. The deposition is made following the protocol used in layer-by-layer deposition of charged macromolecules [63]. In this method, a charged surface is immersed in a solution of species bearing opposite charge. In our case, charged microparticles (made by copolymerization with AMPS) and a polyelectrolyte (PDAMAC) are used. Optical microscopy observation of the samples shows a bidimensional random assembly of microparticles with increasing coverage upon every step (Figure 3a). However, it can be observed that the size of some particles seems to increase with each step, suggesting fusion of the individual microparticles. Using microparticles yellow- and blue-dyed, it can be observed that fused microparticles are formed (Figure 3b).

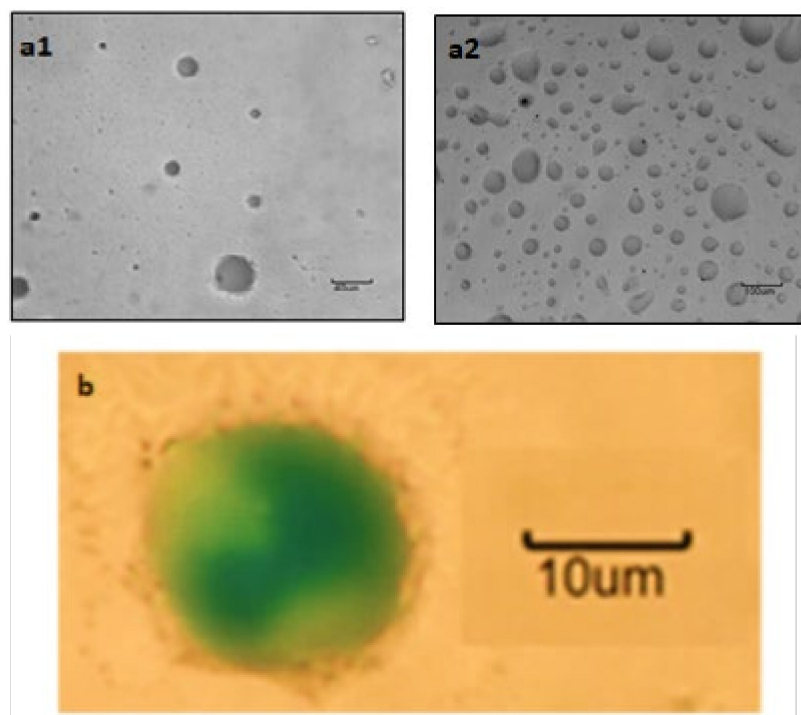


**Figure 3.** Optical micrographs taken during a step-by-step self-assembly of charged (anionic) gel microparticles (poly(NIPAM(0.98)-AMPS(0.2)) with a linear cationic polyelectrolyte (PDAMAC): (a1) after 1 step; (a2) after 5 steps. (b) Self-assembled fused microparticle where yellow- and blue-dyed microgels are used in alternate steps.

As a control experiment, self-assembled layers of charged polystyrene microparticles (Dyospheres<sup>®</sup>) were prepared and showed the same increased coverage with adsorption steps but no coalescence. Unlike hard particles, gels are made of linear chains linked in a network by cross-links. In principle, polymer chain “loops” could entangle, leading to fusion of the microparticles. Indeed, self-healing gels [64] adhere to each other by some strong interaction (e.g., Coulombic attraction), but local interpenetration of the chains is always required. The relevance of the observed “fusion” behavior of gel microspheres to the gel theory of biological cells [65] remains to be seen.

### 3.1.5. Gels as Nanocomposite Matrixes

Gels can act as matrixes of nanoparticles to make nanocomposites. The nanoparticles have to be dispersed uniformly in the gel matrix. The simplest way to insert the particles inside the gel involves absorption. This can be easily performed with macroporous hydrogels since the particles could be transported inside the gel and adsorbed at the pore surfaces. However, macroporous gels are usually mechanically weak due to the large pore volume filled with solution [66]. As it will be seen, this is not the case for cryogelated PNIPAM gels [20]. Another way involves forming the cross-linked gel around the dispersed nanoparticles [42]. The drawbacks of this approach are possible inhibition of the polymerization

process by the nanoparticles (e.g., radical trapping) and aggregation of the particles during polymerization. The latter can be due to the immobilization of water by the growing polymer chains. Finally, those nanoparticles that can be made by soft chemistry could be grown inside the gel matrix. In that way, we made nanocomposites with nanoparticles of metals grown photochemically inside a polyacrylamide gel matrix [29]. We have also made nanocomposites containing PANI and PPy nanoparticles by in situ oxidative polymerization of the monomers (ANI OR Py) inside the gel [13]. It is noteworthy that, usually, these materials have been thought by others [67], and us [13], as semi-interpenetrated networks. The rationale here is that if a linear polymer (e.g., polyaniline) is grown inside a polymer network, the linear polymer interpenetrates the network. While this is likely to be true when polymers, which are soluble in water (e.g., HEMA), are grown inside a cross-linked network [68], it is not true when a polymer insoluble in water, like most conducting polymers, is grown inside a swollen nanoporous gel. Instead, the nanopores are filled up by the conducting polymer precipitate, producing a nanocomposite [19]. Another way to obtain nanocomposites involves the formation of a thermosensitive hydrogel matrix around conducting polymer (CP) nanoparticles. The nanoparticles could be made of any CP nanospheres (e.g., PPy or nanofibers (e.g., PANI) dispersed in aqueous solution. However, the concentration of the initiator has to be larger since the NPs act as traps for the free radicals in the growing chains. Moreover, some aggregation was observed since there was less free water on the growing gel to disperse the nanoparticles.

### 3.1.6. True Semi-Interpenetrated Networks (s-IPN)

As discussed above (Section 3.1.5), the formation of a conducting polymer inside a nanoporous gel forms a nanocomposite. To form a true semi-interpenetrating network (s-IPN), linear CP chains should penetrate the 3D gel network. One way to do that is to absorb soluble polymer molecules into the gel. As it will be discussed below, we found that some polyacrylamides (e.g., PNIPAM) swell strongly in solvents (e.g., NMP), where conducting polymers (e.g., PANI in its emeraldine base form) are soluble [69]. Different polymer domains, clearly seen in the nanocomposite by microscopy, cannot be seen in the s-IPN of PANI loaded inside a PNIPAM gel [19]. Moreover, the LCST of the s-IPN reaches 53 °C (compared with 32 °C for PNIPAM or nanocomposites), suggesting a close contact of PANI and PNIPAM chains. The hydrophilic PANI stabilizes the hydrophilic (coil) form of PNIPAM. Higher temperatures are required to transition PNIPAM to a more hydrophobic (globule) state. Such property changes are a clear evidence of semi-interpenetration but could be a drawback when combined properties are sought. On the other hand, if small nanoparticles of the materials are necessary, the conducting polymer nanoparticles (ca 200 nm) could be too large, and the true s-IPN is the best option. Since the absorption method uses a solution of a preformed polymer, linear polymers, which are difficult to make by soft chemistry (e.g., PET), can be semi-interpenetrated in gels. In that way, we absorb polystyrene from its chloroform solution (which also swells PNIPAM) and improve the mechanical properties of the gel [33]. In Table 1 are summarized the different methods used to produce gels and nanocomposites.

**Table 1.** Fabrication methods of gels and nanocomposites.

Structures	Fabrication Method	Applications	Refs
Nanoporous gel	Radical polymerization with cross-linkers	Thermosensitive gels Cell growth scaffolds Amphiphilic gels Electrochemical sensors	[7,10,11,15,30,31,33,38]
s-IPN	Absorption of true polymer solution	Photothermomechanical actuators Pressure sensors	[19]

Table 1. Cont.

Structures	Fabrication Method	Applications	Refs
Macroporous gel	Cryogelation	Biological cell scaffold Absorption of nanoparticles	[12,20,22]
Macroporous nanocomposite	Swelling the macroporous gel in a dispersion of the nanomaterial.	Photothermomechanical actuators	[12]
Microparticles	Radical polymerization inside water in oil emulsions	Self-assembled monolayers with cell-like fusion	[60]
Nanoparticles	Controlled nucleation and growth polymerization with charged comonomer (e.g., AMPS)	Thermosensitive dispersions	[60,61]
Nanocomposites	In situ formation of nanomaterial (metal, CP) inside the gel	Bactericide (Ag NPs) Pressure sensor (CP)	[13,29,36,43]
Nanocomposites	Formation of gel around the nanomaterial (CP nanoparticles, graphene)	Pressure sensors Photothermal bactericide films Protective carrier of bioactive compounds	[17,18]

### 3.2. Tuning the Physicochemical Properties of the Gels

Cross-linked polymer gels have interesting properties: strong swelling in water and nonaqueous solvents (and its mixtures), critical solution temperatures (LCST), solute partition, mass transport, and mechanical characteristics. Those properties can be tuned by changing the chemical composition (copolymerization), semi-interpenetration, or nanocompositing and changing cross-linking degree and/or porosity. Since being able to finely tune the properties is required for building technological applications of the gels, our efforts to develop such capacities are described.

#### 3.2.1. Swelling in Water

Most of the cross-linked gels swell in aqueous solutions and are termed hydrogels. The swelling is directly related to the solvation of free polymer chain sections (between cross-links) in a solvent, from a compact (“globulelike”) state to a solvated extended (“coil-like”) state. The driving forces of solvation are the interactions of the solvent molecules with the polymer chains and the increased conformational entropy of the polymer chain in solution. Against the solvation are the chain-to-chain interactions and the rigidity of the chains. The latter factor is observed in gels as an elastic force. Being polyacrylamide vinyl polymers (with free rotation of C–C bonds), they are flexible, but the functional groups attached to the acrylamide group could hinder the rotation of C–C linkages. This can be performed by making larger the attached group, increasing the excluded volume, or by introducing immobile charges in the hanging groups, inhibiting the approach due to Coulombic repulsion. By copolymerization of different acrylamides, it is possible to introduce hydrophilic groups (e.g., -OH), which interact with water (hydrogen bonding), increasing the swelling degree [44]. Moreover, polyacrylamides containing charged groups belong to the so-called superabsorbent materials, where the gels swell to a large degree (>10.000%) in water mainly due to the osmotic pressure exerted by the mobile counterions of the charged group inside the gel matrix. Water enters the gel to decrease the concentration of ions inside the gel until the chemical potential is balanced. The pressure exerted inside the gel expands it to large volumes. However, the osmotic pressure depends on the ionic strength. Usually, swelling is measured in pure water, but in technological applications, such as biological media, the solution has large ionic strength. We measured such effects

and found that swelling in biological media is significantly smaller than in pure water [27]. Using a combinatorially synthesized library of 21 hydrogels (made by combining 6 different acrylamides) [26], it was noticed that the swelling degree could be related to the properties of the functional groups present in the chain. The need to copolymerize 21 different monomer mixtures allows for testing the hypothesis that all acrylamide polymerization is the same. In fact, it was found that some monomer mixtures do not give mechanically stable materials, and changes in the polymerization conditions (increased total monomer concentration, use of thermal instead of redox initiation) were required. Therefore, the typical methods of radical polymerization of acrylamides (redox initiation, 1 M or lower monomer concentration, 2% (molar) amount of cross-linker, room temperature) are not always useful, and it has to be tested in each case. As expected, the gels containing hydrophilic groups, being neutral (-OH in HEAA) or charged ( $-\text{SO}_3^-$  in AMPS or  $-\text{N}(\text{CH}_3)_4^+$  in APTMAC), show large swelling degrees. Accordingly, swelling at equilibrium goes from 703 (PAA) to 34,403 (PAMPTAC). The experimental swelling can be changed extensively by copolymerization of monomers bearing different groups. Since all copolymers are made with a 1:1 monomer ratio, it is possible to estimate the contribution of each functional group to the swelling. It is found that swelling degrees differ from the average value calculated from the swelling of the homopolymers, suggesting that interactions between neighboring functional groups exist. A clear case is P(AMPS-co-AMPTAC), where a large (>1200%) departure from the average swelling, expected by the contribution of each charged group (ion-dipole interaction), is observed. It is likely that an inner salt (zwitterion) is formed, which creates an extra chain-to-chain interaction opposing the expansion during swelling. However, in other cases, like P(AAm-co-50%HEAA), the swelling is larger (+49%) than the average, suggesting a synergic effect of the two hydrophilic neighboring groups to intake water, while intrapolymer hydrogen bonding interactions between chains could be expected. The swelling is mainly driven by water interaction with polymer chains (fixed water). However, being a tridimensional network makes that expansion create a porous volume, which is filled with free water. One way to measure the relative amount of fixed to free water is monitoring the melting of frozen water by differential scanning calorimetry (DSC). Fixed water melts at a lower temperature due to colligative properties. From the area of DSC profiles, and the  $\Delta H_{\text{melting}}$  of water, the relative amount could be calculated. In general, the water structure in the polymer hydrogel can be categorized as “free water”, “strongly bound water”, and “weakly bound water”. Free water is incorporated by mechanical suction and is not interacting with the polymer chains. It behaves like pure water regarding melting temperature and enthalpy, giving the same DSC curve as that of pure ice. Strongly bound water (nonfreezing,  $w_{\text{nf}}$ ) is the fraction of water that forms hydrogen bonds with the polymer chains and could not freeze/melt because it is not mobile. Weakly bound water (freezing,  $w_{\text{f}}$ ) interacts weakly with polymer chains. It can freeze/melt because it is mobile but shows colligative properties different than that of pure water. The total content of freezing water ( $w_{\text{f}}$ ) was calculated using DSC, from the area under the curves of the melting peaks and the  $\Delta H_{\text{melting}}$  of water (Table 2).

**Table 2.** Effect of copolymer composition and fabrication method on the amount of freezing and nonfreezing water (measured by DSC).

Composition (% in Feed)		Nanoporous		Macroporous	
NIPAM	Comonomer	$w_{\text{nf}}$ (%)	$w_{\text{f}}$ (%)	$w_{\text{nf}}$ (%)	$w_{\text{f}}$ (%)
100	0	34.5	62.9	18.5	76.9
90	HMA (10%)	60.3	30.5	50.6	45.4
98	AMPS (2%)	55.1	42.7	2.4	94.7

In both PNIPAM and P(NIPAM-co-2%AMPS), the percentage of freezing water (free and weakly bonded) is larger in the macroporous gels, where the macropores are filled

with water not interacting with the polymer. Therefore, the mental image of a gel as a sponge is partially true for macroporous gels but not true for nanoporous materials. On the other hand, in both the macroporous gel of P(NIPAM-co-10%HMA) (spherically closed cavities) and all the nanoporous gels, the percentage of freezing and nonfreezing water is similar [20]. However, hydrogels show slow swelling until the equilibrium is reached. The kinetics of water intake is related to the balance of the driving force: osmotic pressure and the opposing elastic force. As can be seen below, macroporous gels show a larger elastic modulus than it could be expected by the large amount of free volume.

### 3.2.2. Swelling in Nonaqueous Solvents (and Mixtures)

Polyacrylamides form acceptor (at carbonyl and nitrogen) and donor (at N-H) hydrogen bonds with water. Other protic solvents (e.g., alcohols) could also form the same kind (while likely weaker) hydrogen bonds. Accordingly, there are several studies on the swelling of polyacrylamides in solutions of organic solvents and water [70–72]. In fact, we used such effects to load phenanthroline, which has low solubility in water, from 70% ethanol solution (which swells PNIPAM). On the other hand, plain polyacrylamide is only slightly swelled in pure ethanol [25] and does not swell in other nonaqueous solvents, suggesting that amide–amide interactions are too strong to be dislodged by solvents, which interact far weakly than water with the polymer chains. There are few studies on the swelling of polyacrylamides in pure organic solvents [73,74]. We explore the absorption of different solvents in PNIPAM [30,33]. The absorption (mole/kg) of different solvents (Figure 4A) is maximum for water and alcohols, likely due to hydrogen bonding of the -OH group with the amide group. Absent strong hydrogen bonding, the absorption seems to correlate with the dielectric constant of the solvent since dichloromethane ( $\epsilon = 10.8$ ) has an absorption of ca. 0.27 moles/kg, while chloroform ( $\epsilon = 4.8$ ) [75] shows a lower absorption of ca. 0.2 moles/kg.

While PNIPAM absorbs short chain alcohols, the equilibrium absorption degree (AbsCap) decreases with the chain length. Amides (including lactams, such as NMP) are absorbed into PNIPAM, likely due to strong hydrogen bonding between carbonyl and N-H groups. The fact that some solvents (e.g., chloroform), which are immiscible with water, are absorbed into the polymer allows building two liquid-phase systems inside a solid PNIPAM [30]. On the other hand, as can be seen in Figure 4A, low-polarity solvents (e.g., toluene) do not absorb in PNIPAM. If two solvents are immiscible (e.g., toluene/water), still homogeneous mixtures (in some molar fraction range, as shown in Table A1 of Appendix A) can be made by mixing with a third solvent, which is miscible with both of them (e.g., ethanol). The absorption of the homogeneous mixture in PNIPAM is shown in Figure 4B. Surprisingly, the mixtures with a larger molar fraction of water (0.634, 0.01 molar fraction of toluene) show small absorption (ca. 0.27 moles/kg), similar to the value for the smaller molar fraction of water (0.04) and larger molar fraction of toluene (0.7). At an intermediate toluene molar fraction, the absorption is higher and follows a regular decreasing trend, which ends in pure toluene with zero absorption. From a practical point of view, it is possible to absorb a mixture that contains a large molar fraction of toluene (a low-polarity solvent).

Using this property, small nonpolar molecules (e.g., iodine) or macromolecules (e.g., polystyrene), which are insoluble in water but soluble in toluene, can be loaded inside PNIPAM gels [30]. Obviously, the same can be done with more hydrophobic gels (e.g., cross-linked PMMA), but here, the gel is amphiphilic. That is, PNIPAM loaded with PS could be dried and then swell in water. In that way, new s-IPN are made with better mechanical properties than pure PNIPAM [30]. Likely, hydrophobic drugs (e.g., doxorubicin) can be loaded into PNIPAM and then released in aqueous solution from the swollen gel.

The swelling half time (inversely related to the rate) is linearly dependent on the viscosity of the solvent. This is interesting since it implies that the elastic forces in the polymer chains are not affected by plasticizing, and the mass transport through the nanoporous matrix is the dominant phenomenon [30].

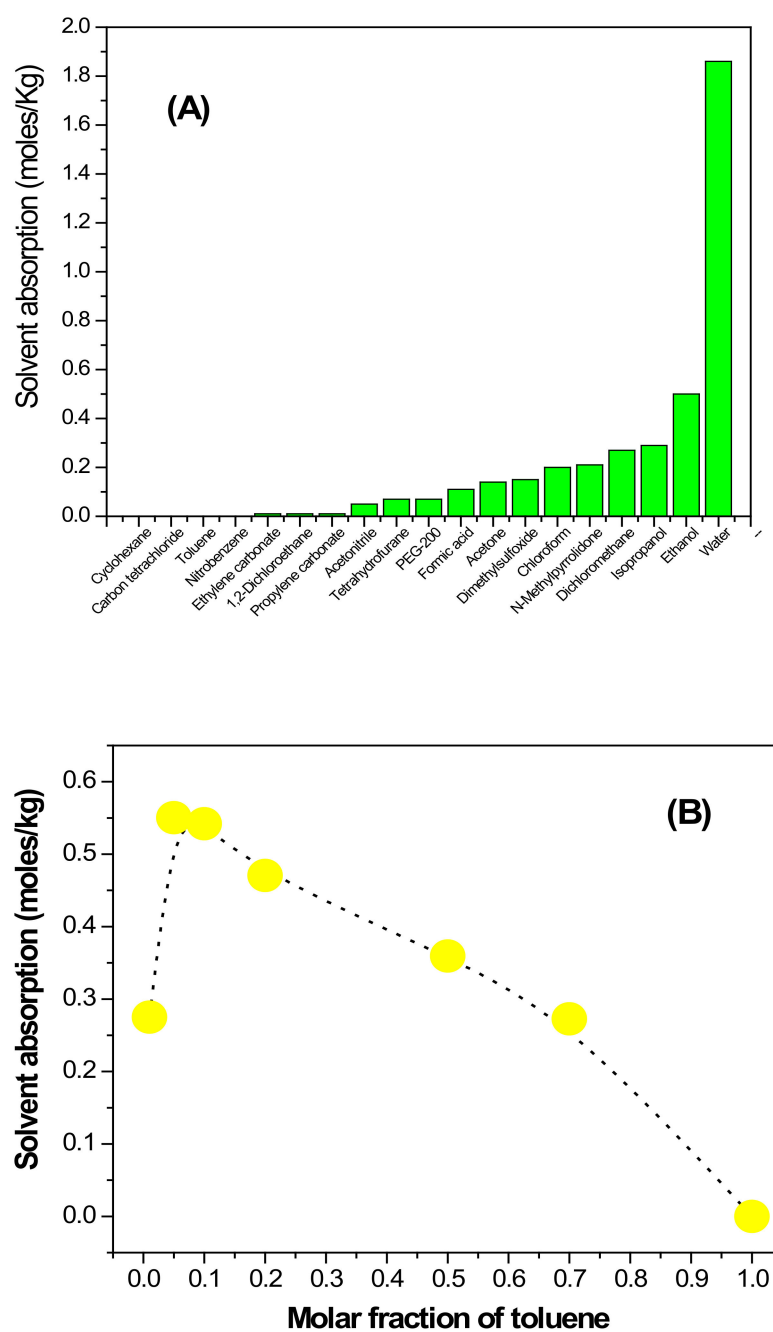


**Figure 4.** (A) Absorption (moles of solvent per kg of dry gel) of different solvents in PNIPAM. (B) Absorption (total moles of solvents per kg of dry gel) of a ternary mixture (water/ethanol/toluene) in PNIPAM gels. The composition of each ternary mixture is described in Table A1 (Appendix A). The dotted line is a guide to the eye.

### 3.2.3. Lower Critical Solution Temperatures (LCST)

The amide groups present in the main chains of the gels interact with water through hydrogen bonding of the carbonyl ( $>C=O$ ) and nitrogen ( $>NR_1R_2$  (with  $R_1 = H$ , alkyl, aryl)). However, the water molecules interacting with the nitrogen could be dislodged by the exclusion effect of alkyl groups bonded to the nitrogen. Specifically, the isopropyl group (present in the NIPAM monomer unit) shows an excluded effect, which depends on the temperature. Above a certain temperature (LCST), the material has enough energy to overcome the activation energy for the rotation around the C–N bond. Additionally, increasing the temperature makes the water molecules more mobile, breaking the hydrogen bonds with the amide groups. Such molecular phenomena make the chains less hydrophilic. Since the



amide groups could also make hydrogen bonds between them (present in different chains or in the same chain), a coil-to-globule transition is driven by the temperature. In a linear soluble chain, it is called a lower critical solution temperature (LCST) since the polymer is soluble below the temperature and insoluble above it. In poly(*N*-isopropylacrylamide) (PNIPAM), the phenomenon has been thoroughly studied [7,76] and used in different technological applications [77]. In pure water, the transition temperature is 32–33 °C. The transition occurs below the human body temperature (HBT, 36.5–37 °C) [78]. Therefore, it cannot be applied to detect (and act) an increased temperature (fever) due to a sickness. Since the LCST depends on the local water activity and the strength of hydrogen bonding between amide groups, introducing a hydrophilic group (e.g., -OH) in the polymer chains by copolymerization increases the LCST. We used the effect to fine-tune the temperature around the HBT [20]. As can be seen (Figure 5), 2% of a charged group (-SO<sub>3</sub><sup>-</sup> in AMPS) changes the LCST of PNIPAM almost in the same degree than 10% of a neutral hydrogen bonding group (-OH in HMA). Groups that form hydrogen bonds with water (e.g., -OH) are effective to increase LCST. However, the addition of charged groups, which has ion–dipole interactions with water and also osmotic pressure from mobile counterions, has an even stronger effect. In any case, it is possible to fine-tune the LCST of the PNIPAM to the HBT with 7% of HMA.

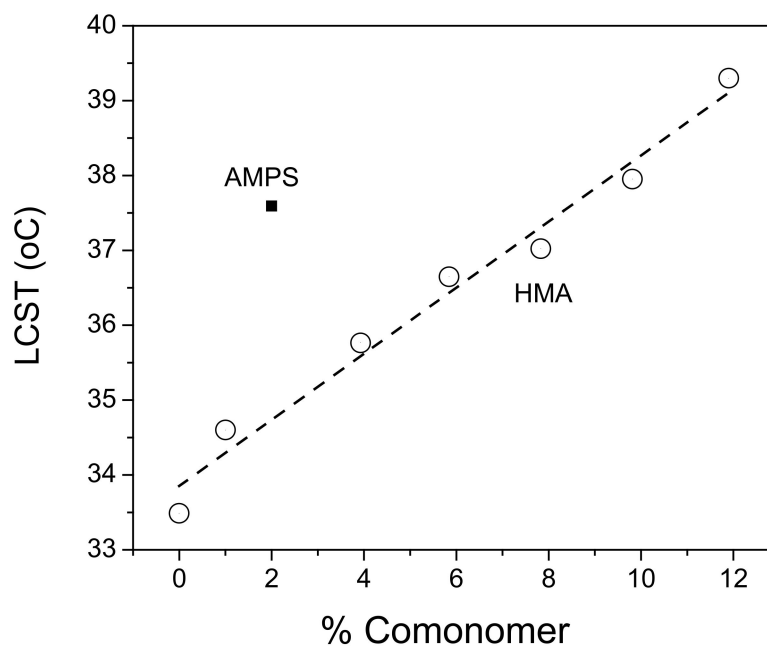


**Figure 5.** Effect of copolymer composition on the LCST of PNIPAM-based materials. Open circles correspond to P(NIPAM-co-*x*%HMA) (*x*% is the percentage of comonomer) while the filled square corresponds to P(NIPAM-co-2%AMPS).

It is noteworthy that both AMPS and HMA are in fact functionalized NIPAM. Copolymerization with a less similar group (e.g., AAm) does not obey such simple model. The effect of hydrophilic/hydrophobic groups on the LCST is usually explained by interactions of the hydrophilic/hydrophobic added groups with the thermosensitive *N*-isopropylacrylamide group. However, it seems that long-range effects, involving several monomer units, are operative. This is reasonable since it is a coil-to-globule transition that requires a minimum chain length to form the structure. From our data, the absence of breakpoints in the relationship between copolymer composition and LCST supports the same mechanism. It is noteworthy that the composition values are calculated assuming that they are the same that feed ratios. It is assumed that the reactivities of NIPAM and other comonomers (e.g., AMPS) to radical polymerization are the same. This is reasonable since electronic effects on the acrylamide group are weak. However, even if both comonomer

reactivities are the same, it only means an alternate copolymer when the ratio is 1:1. In other cases, like those described in Figure 1, a small amount of the acrylamide monomer containing a hydrophilic/hydrophobic group is added, and random block copolymers are made. Therefore, not only neighboring groups affect the LCST, but neighboring blocks of active groups change the LCST of the NIPAM blocks. Moreover, incorporating a hydrophilic polymer (e.g., PANI) as a semi-interpenetrated linear polymer in the gel network, made by swelling the gel in a true solution of PANI in NMP, significantly increases the LCST [19]. However, when the same polymer is present in nanometric domains, made by in situ polymerization/precipitation [13], or by entrapment of preformed nanoparticles inside the gel [42], negligible changes in LCST are observed. The LCST is a molecular phenomenon and occurs in bulk hydrogel (e.g., a cube of 1 cm per side) [13], but also in small nanogels (Figure 6). The hydrodynamic radius decrease by ca. 66% upon heating the solution.

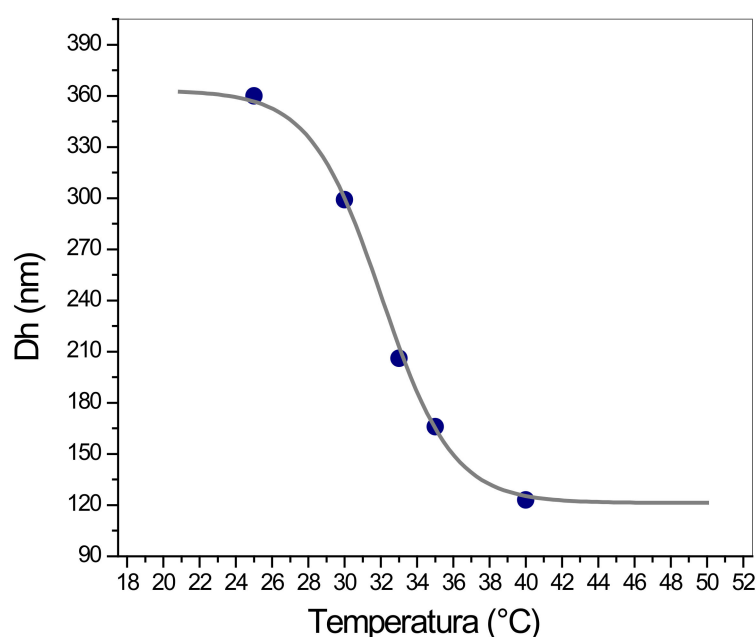


**Figure 6.** Effect of temperature on the hydrodynamic radius (measured by DLS) of cross-linked P(NIPAM-co-2%AMPS) nanoparticles.

An interesting point is that the LCST of the nanogels in Figure 6 is ca. 32–33 °C, lower than for bulk P(NIPAM-co-AMPS) (37.6 °C) and similar to PNIPAM. It seems that AMPS is less reactive than NIPAM, and the core of the nanogel is richer in NIPAM, while the compositional shift makes the shell of the nanogel rich in AMPS. Such compositional gradient is positive to the stabilizing effect of the  $-\text{SO}_3^-$  group on the colloid, but it should be taken into account when attempting to tune the LCST of nanogels by copolymerization.

#### 3.2.4. Solute Partition

Hydrogels contain a large amount (>70%) of water inside the porous matrix. In most published works, it is implicitly assumed that, absent immobile charge effects, the relative amount of ions dissolved inside the gel is the same as in the bathing solution. We have shown that this is not the case for PNIPAM and its copolymers [13]. A likely reason is the interaction of the solvated ions with the polymer chains. Even in the absence of specific interactions (hydrogen bonding, Lewis acid/base, Coulombic), van der Waals (hydrophobic) interactions could account for the retention of large ions inside hydrogels [20]. The incorporation of other polymers, with their own hydrophilic/hydrophobic properties, inside the pores also affects the partition equilibrium of solutes [20]. We measure the effect of copolymerization and semi-interpenetration on the spontaneous release of a model colored ruthenium complex: Rubipy [20]. The amount of Rubipy released from the hydrogel

was measured by spectrophotometry in the solution. The amount of Rubipy decreases as the percent of AMPS increases (in the series, PNIPAM, P(NIPAM-co-2%AMPS), and P(NIPAM-co-20%AMPS)). It seems that Rubipy, being positively charged, interacts Coulombically with the negatively charged sulfonate groups (from AMPS). Upon loading the gel with conducting polymers (PANI or PNMANI), the amount of Rubipy released from P(NIPAM-co-AMPS) increases. The amount of Rubipy released is also larger when conducting polymers are loaded in neutral PNIPAM gel; therefore, electrostatic interaction with the sulfonate group is not causing it. Moreover, PNIPAAm-co-20%AMPS/PANI releases six times more Rubipy than PNIPAAm-co-20%AMPS. It seems that the presence of the conducting polymer in the material induces an additional hydrophobic effect, which helps increase Rubipy loading. Accordingly, the effect is stronger when PNMANI (less hydrophilic [79]) is loaded instead of PANI (more hydrophilic). We know now that the hydrogel/conducting polymer materials are nanocomposites (two solid phases) and not s-IPN (one solid phase), and it seems that Rubipy is retained in the conducting polymer domains by hydrophobic interactions. Since PNIPAM shows an LCST, when the gel collapses, expelling solution, and becomes less hydrophilic, it is possible to study the release of Rubipy driven by temperature changes. The usual view of thermosensitive gels is that they are sponges filled with solution that collapses above the LCST, releasing the inner solution, like a sponge squeezed. However, in Figure 7, it can be seen that this seems to be true for PNIPAM itself, where the Rubipy absorbance (outside the gel) *INCREASES* above the LCST (solute release).

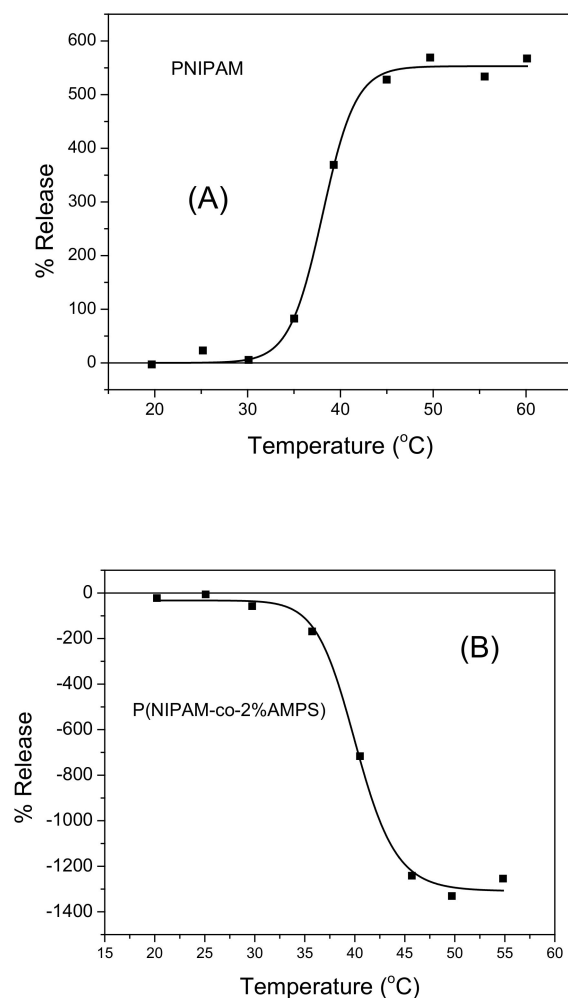


**Figure 7.** Rubipy release (measured by spectrophotometry in the solution side) from gels at different temperatures. (A) PNIPAM. (B) P(NIPAM-co-2%AMPS).

On the other hand, incorporating only 2% of AMPS changes the properties of the gel, and the Rubipy absorbance *DECREASES* in the outer solution (solute intake) above LCST. It should be noted that above an LCST, PNIPAM becomes more hydrophobic. The combination of the Coulombic attraction of the positive charges in Rubipy with the  $-\text{SO}_3^-$  group (in AMPS) with the increased hydrophobic interactions means that Rubipy is taken in instead of released. To find the best gel for the retention of iron(II) complexes, a combinatorial library of hydrogels (21 different copolymers) was made and tested using a colorimetric high-throughput screening (HTS) [26]. The partition coefficient of  $\text{Fe}^{2+}$  and  $\text{Fe}(\text{Phen})_3^{2+}$  in all hydrogels is determined by UV-VIS spectrophotometry (in the solution). Hydrogels containing sulfonic ( $-\text{SO}_3^-$ ) groups (from AMPS) show large values of partition coefficients (Pc) of  $\text{Fe}^{2+}$  into the hydrogel ( $>500$ ). P(AAm-co-AMPS) shows a partition coefficient of 1009. Since phenanthroline is only slightly soluble in water, the complexing agent is loaded from a solution in 70% ethanol, where PNIPAM shows maximum swelling. Interestingly, in the case of PNIPAM, the loading of Phen decreases the Pc by 286%, while for p(NIPAM-co-AA), the Pc increases by 515%. Taking into account the partition coefficients, some materials (e.g., P(AAm-co-50%AMPS)) could be used both to retain free iron and to detect iron through the formation of the colored iron-phenanthroline complex due to the large Pcs. In the case of neutral hydrophilic active agents (phenolic antioxidants), it was found that more hydrophilic gels (P(NIPAM-co-8%HMA)) retain and release more substance [44].

### 3.2.5. Mass Transport of Mobile Species

Small molecules (e.g., water) or ions (e.g.,  $\text{Na}^+$ ) can permeate through the nanoporous structure of gels. Mass transport could only occur by diffusion or migration, not convection. Spontaneous release of a molecule/ion loaded inside a gel, which is in swelling equilibrium, to a solution occurs through diffusion since no electric field is applied to induce migration. The magnitude of diffusion coefficients for mobile species inside the gels is ca. 3 orders of magnitude (ca.  $10^{-8}$   $\text{cm}^2/\text{s}$ ) smaller than those measured in diluted aqueous solution (ca.  $10^{-5}$   $\text{cm}^2/\text{s}$ ). Therefore, the release is controlled by the mass transport inside the gel. The amount of substance released at a given time ( $M_t$ ) is related to the equilibrium value ( $M_\infty$ ) by Equation (4):

$$\left[ \frac{M_t}{M_\infty} \right] = k t^n \quad (4)$$

where  $n$  is the order of the process. If a gel slab is used, where the thickness is smaller than the dimensions of the exposed area,  $n$  should be 0.5. In the case of the more practical cylindrical slab,  $n = 0.45$ . This is called Fickian diffusion. In drug release, usually the loaded hydrogel is not swollen, swelling and diffusion occur simultaneously, and anomalous behavior ( $n > 0.45$  or  $n < 0.45$ ) could be observed. In any case, the mass transport could be changed by changing the porosity of the gel. Additionally, interactions of the mobile species (Coulombic attraction, hydrogen bonding, and hydrophobic attraction) could decrease the diffusion rate. The effect of a copolymeric composition on the diffusion rates for colored ions (using spectrophotometry to determine the concentrations) was studied. Using hydrogel cylinders, both normal and anomalous behaviors were found [15]. Using thin hydrogel slabs, normal diffusion was observed [26]. Neutral organic substances (phenolic antioxidants) show diffusion coefficients inside neutral copolymers (e.g., P(NIPAM-co-8%HEA)) ranging from 1 to  $100 \cdot 10^{-7}$   $\text{cm}^2/\text{s}$  [44]. Dynamic electrochemistry could be used to study mass transport (diffusion and migration) in liquid solutions [80]. However, since a solid electrode is used in the measurements, hard solid cannot be used as electrolyte unless both solids are compacted to a sharp interface. While electrochemistry has been widely used to drive polymerization reactions for the fabrication of nanocomposites [81], it is seldom used to sense ions inside bulk preformed gels. It was found that a simple flat solid electrode, pressed onto a wet bulk gel, gives a good interface to perform electrochemical measurements. Again, these results support the existence of a liquidlike interface in the gel surface. First, hydrogels containing at least 10% of charged monomer units show only diffusion control of mass transport (no migration) found. Accordingly, the time response

obeys the same equations (e.g., Cottrell) than redox species in dilute solution of electroactive species in a supporting electrolyte (>10 times concentration of an inert salt (e.g., KCl)). The diffusion coefficients are small ( $10^{-9}$ – $10^{-8}$  cm<sup>2</sup>/s), as expected for compact gels, depending on the copolymer composition, and their values are related to the swelling rates. That is, gels that swell slowly due to large elastic modulus show lower diffusion coefficients and vice versa. Charge transfer effects occurring at the electrode/gel interface also depend on the chemical composition and, according to Marcus theory [82], scale inversely with the local mobility (diffusion coefficient). This result suggests that the electrode/gel interfaces show no defects. If a thin layer of solution would be present at the interface, the charge transfer constant would be the same (that of the bathing solution) for all gels. Interestingly, in solid polymer electrolytes, Donnan exclusion is assumed to be operative for low ion strength solutions. This means that mobile counterions (opposite charge of the fixed charges) are extracted to the gel, while mobile co-ions (same charge as the fixed charges) are excluded. Such effect is the rationale to use charged hydrogels to extract toxic ions from solution [83]. However, we found what could measure electrochemical responses of redox negatively charged ions (e.g., Fe(CN)<sub>6</sub><sup>−3</sup>) loaded inside negatively charged hydrogels (poly(NIPAM50%-co-AMPS50%)) and redox positively charged ions (e.g., FePhen) loaded inside positively charged hydrogels (poly(NIPAM50%-co-AMTAC50%)). These results show that gel matrixes, with a large amount of free solution inside the pores, are different from more compact polyelectrolytes (e.g., Nafion<sup>®</sup>) where Donnan exclusion is operative [84].

### Mechanical Properties

Cross-linked polyacrylamides are quite soft materials since the linear chains (between cross-links) are constituted by C–C bonds that can take different conformations. Moreover, the nanopores are free space for chain mobility. Decreasing mobility by the incorporation of large pending groups (steric effects) or charged groups (Coulombic repulsion) makes the gels more rigid. In that way, we found that a macroporous P(NIPAM-co-10%HMA) gel (closed spherical pores) has lower elastic modulus than the nanoporous gel of the same composition (Table 3). On the other hand, for PNIPAM and P(NIPAM-co-2%AMPS), the oriented cryogelation renders pores with a large aspect ratio [20].

**Table 3.** Effect of copolymer composition and fabrication method on the elastic modulus of the material.

Composition (% in Feed)		Elasticity Modulus (kPa)		
NIPAM	Comonomer	Nanoporous	Macroporous (Collinear)	Macroporous (Transversal)
100	0	5.9	33.3	10.9
90	HMA (10%)	5.9	3.1	3.1
98	AMPS (2%)	6.6	20.5	12.1

It was observed that macroporous gels, with oriented macropores made by cryogelation, show anisotropy with the material more rigid in the same direction of the pores than transverse to it (Table 1). It seems that the pore walls are made of a more rigid material than the nanoporous gel, likely due to the special conditions of polymerization during cryogelation, where the concentration of the reactants is higher due to the solvent (water) freezing. Filling the nanopores with a more rigid polymer (e.g., PANI) also increase the elastic modulus. By simultaneously measuring stress–strain curves and resistance, it is possible to determine the gauge factor, which is the relationship between pressure and conductance. It was found that the gauge factor of a nanocomposite of a conducting polymer (polyaniline) inside a gel (PNIPAM) is ca. 9 times larger than for a semi-interpenetrated network of the same components. It seems that the electrical contact between nanoparticles increases strongly by compression. On the other hand, the s-IPN behaves as a homogenous material, where the gauge factor is related to the decreased length of the conductor. Another

nanocomposite with similar properties was made by polymerization of the hydrogel matrix around graphene oxide nanoparticles [35].

### 3.2.6. Hydrophilicity

Polyacrylamide hydrogels are intrinsically hydrophilic since water interacts strongly with the amide groups by hydrogen bonding. However, the hydrophilicity could be reduced (e.g., by incorporating monomer units with pending alkyl groups) or increased (e.g., by adding -OH groups). Since several biological phenomena, such as cell adhesion and differentiation, could be directly related to the hydrophilicity, the ability to tune it is of great importance. The most widely used method for determining hydrophilicity is water contact angle. The measurement is complex in gels since only gels completely swollen in water can be used. However, large trends are evident. Copolymerization of NIPAM with AMPS renders a gel more hydrophilic. Moreover, nanocompositing of PNIPAM with PPy (a conducting polymer less hydrophilic than PANI) gives a less hydrophilic material [27].

### 3.2.7. Photothermomechanical Behavior

Several gels (e.g., PNIPAM) show large volume changes at a given temperature (LCST). Light in the visible–NIR range does not affect the gel. However, loading the polymer with light absorbing molecules allows for reaching the LCST by thermalization of the absorbed light. A NIR dye (IR800) is absorbed by swelling a PNIPAM gel in a chloroform solution of the dye. The solvent is then evaporated, and the modified gel swollen in water. Upon irradiation with NIR light (808 nm), the gel reaches the LCST and collapses. Moreover, the dye could be loaded in only half of the gel by swelling the gel in a water/chloroform biphasic system. After drying and swelling in water, a half-colored cylinder is made. Upon irradiation with NIR light, only the dyed part collapses [30], supporting the model of a local phenomenon. Since conjugated polymers (e.g., PANI) have electronic transitions that absorb light in NIR, it is possible to heat up the PANI by light and drive the LCST of PNIPAM. PANI (base form) can be semi-interpenetrated in PNIPAM gels from its solution in NMP, but the s-IPN has a higher LCST (53 °C) due to the hydrophilic effect of PANI [19]. On the other hand, PANI nanoparticles can be formed inside gels by in situ polymerization [19]. Accordingly, the nanocomposite suffers a volume collapse when reaching the LCST of PNIPAM (32 °C) by thermalization of NIR light. Being conductive, PANI could also be heated by oscillating electromagnetic fields, such as those existing in microwaves (e.g., 2.4 GHz) and RF (30 kHz). The oscillating fields interact with the electronic conductor (PANI), inducing eddy currents, which heat up the PANI by the Joule effect [13]. The heat increases the temperature of the whole nanocomposite film, driving the phase transition of the PNIPAM matrix. It could be envisaged that at least microwaves do not require PANI to be conductive and are absorbed in the dipoles existing in the conjugated polymer. To try to find the mechanism, the nanocomposites are immersed in a solution of basic pH. PANI becomes deprotonated and nonconductive but retains optical absorption in the NIR. When the treated nanocomposites are tested, it is found that NIR light still is able to drive the LCST transition, but microwaves and RF do not cause any volume change. The temperature, measured with an IR camera, shows that only NIR light is able to heat up the material supporting the mechanism proposed [41]. Other nanocomposites are like those containing PPy nanoparticles [13]. PANI nanoparticles absorbed in macroporous PNIPAM gels [12] or trapped inside the growing gel by in situ polymerization [42] show similar photothermomechanical effects. Thin films of the nanocomposites structured by DLIP also show changes in topography when subjected to RF [42]. Besides bulk nanocomposites, PANI nanoparticles stabilized with thermosensitive polymers (PNIPAM and HPC) aggregate when illuminated with NIR light [49]. The aggregation occurs because the heat, produced by thermalization of NIR light, induces the coil-to-globule transition of linear PNIPAM, adsorbed on the surface of PANI nanoparticles. The globular form of PNIPAM does not interact with water enough to stabilize the dispersions. The smart nanoparticles themselves could be used to stabilize Pickering emulsions of liquids immiscible with water. Upon irradiation with

RF, the emulsion is un-stabilized, and the oil drops coalesce [45]. Finally, the smallest PANI-PNIPAM nanocomposite is made by synthesizing a block copolymer (PNIPAM-*b*-PANI). The copolymer is soluble in aqueous solution, unlike PANI, due to the interaction of PNIPAM extended chains with water. Upon irradiation with NIR light, the PANI block heats up and drives the coil-to-globule transition of the PNIPAM block. Therefore, the macromolecules aggregate and precipitate. A monolayer of the copolymer suffers a volume change in the region illuminated by light, which is detected by AFM [39].

### 3.3. Applications

#### 3.3.1. Drug Release

Since hydrogels should be in equilibrium with the surrounding solution, a hydrogel loaded with a chemical absent in the solution will spontaneously release it by diffusion. The release of common bioactive compounds (tryptophan, propranolol, riboflavin) was studied [20]. Nanocompositing with PANI, the PNIPAM-based hydrogels allow increasing the loading capacity to small drugs (propranolol, riboflavin, and tryptophan). Large partition coefficients ( $\log K > 3$ ) are measured for neutral molecules. The compounds release could also be driven by volume collapse related to the LCST transition. The release of phenolic antioxidants from hydrogels was studied. A slow (long term) release is observed for hydrophilic matrixes, such as PNIPAM-co-8%NAT, while a fast (short term) release is shown in less hydrophilic matrixes as PNIPAM. The released antioxidants show activity against photogenerated reactive oxygen species in aqueous solution [44]. For nanocomposites of PANI with PNIPAM, the release could be also driven by the absorption of electromagnetic radiation (e.g., microwaves) [20]. It is noteworthy that the volume collapse is not the same as a sponge squeeze, but the collapsed state is less hydrophilic than the expanded state. Therefore, hydrophobic species (e.g., Rubipy) will not be released but taken at temperatures above the LCST.

#### 3.3.2. Actuators

As discussed above, some acrylamides suffer a phase transition at its LCST, decreasing its volume. This change can be used in thermomechanical actuators. However, this can only be performed with thermal contact with the sample. On the other hand, if electromagnetic radiation (e.g., light) is absorbed in the material, it is possible to heat it remotely. Conducting polymers (e.g., PANI) are highly colored and can be heated by irradiation with light. Specifically, they absorb in the near-infrared region (700–1200 nm) where biological tissue has its lowest absorption, allowing the radiation to be applied through massive tissue. Combining the absorption of PANI with the thermosensitivity of PNIPAM, at close contact between them, it is possible to make a photothermomechanical actuator. The simplest way to perform that is to produce a nanocomposite by in situ polymerization of aniline inside the PNIPAM hydrogel [13]. Other nanocomposites were developed by absorption of PANI (or PPy) nanoparticles inside macroporous PNIPAM based gels [12], or polymerization of the gel around dispersed PANI nanoparticles [42]. On the other hand, a true semi-interpenetration of PANI in PNIPAM by swelling the latter in a solution of PANI in NMP renders a material with photothermal properties, but the LCST is also increased. Smaller systems involve PANI nanoparticles stabilized with PNIPAM, where PNIPAM linear chains suffer a coil-to-globule transition and diminish its stabilizing effect upon irradiation, inducing nanoparticle aggregation [49]. The smallest photothermomechanical actuator was made by linking single PNIPAM and PANI chains (block copolymer). Again, the PANI chains absorb NIR light and heat the PNIPAM chains, triggering the transition to its globule form. The clear green solution becomes opaque after irradiation. Since PANI and PPy are conductors, nonoptical electromagnetic radiation is not absorbed but induces eddy currents inside the conducting polymer domains. Those currents heat up the polymer by Joule effect. Therefore, other electromagnetic radiations, such as radiofrequency (RF, 30 kHz) and microwaves (2.4 GHz), can drive photothermomechanical actuators. In that sense, a microwave-driven actuator could open a contact [16]. RF is used to switch states in

a structured surface of PNIPAM loaded with PANI [42]. A similar approach uses PNIPAM to stabilize Pickering emulsions, which can be destabilized (“broken”) by the application of heat or microwaves [45].

### 3.3.3. Sensors

One kind of electrochemical sensors uses reversible redox couples as redox catalysts of irreversible electrochemical reactions. An analytically interesting ion (e.g., nitrite) shows slow electrochemical oxidation (charge transfer) on glassy carbon electrodes. Therefore, a reversible couple (e.g.,  $\text{Fe}(\text{phen})_3^{2+}/\text{Fe}(\text{phen})_3^{3+}$ ) could be used to catalyze the reaction. The reduced form of the complex is oxidized in the electrode, giving an electric signal to its oxidized form, which is reduced by the analyte (nitrite). In that way, the electric signal is proportional to the concentration of nitrite. While such method is widely used with the indicator molecule in solution, applying a gel has several advantages. First, the analyte could be concentrated inside the gel (compared with its concentration in solution) due to a positive partition equilibrium driven by interactions between the gel and the analyte. Second, the nanoporous gel could act as a filter of other redox species present in the sample (e.g., blood), allowing measurement without interference. Third, the indicator could be mechanically removed from the solution. A disadvantage is that the analyte has to diffuse inside the gel, a slow process. Again, the use of gel structures with shorter diffusion lengths (microparticles, nanoparticles, thin films, macroporous monoliths) allows for a fast response. Since swollen hydrogels are transparent, they can be used as colorimetric sensors of ions. Loading a complexing agent inside the gel, retained by hydrophobic interactions, allows for detecting specific ions by the formation of colored complexes (Figure 8).

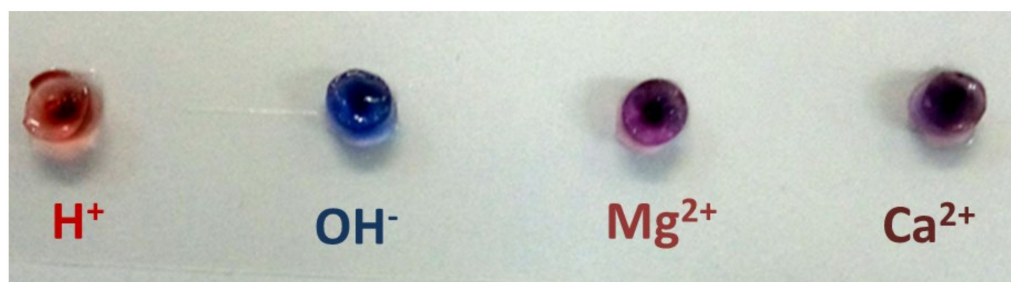


**Figure 8.** Photographs of PNIPAM gels loaded with a complexing agent (EBT), then dried and swollen to equilibrium in: acid media ( $\text{H}^+$ , pH = 1), basic media ( $\text{OH}^-$ , pH = 9),  $\text{Mg}^{2+}$  solution (1 mM, pH = 9),  $\text{Ca}^{2+}$  solution (1 mM, pH = 9).

Since the complex of iron with some complexing agents (Phen, Bphen) is colored, the presence of  $\text{Fe}^{2+}$  in the solution can be visually detected. A PNIPAM/BPhen gel shows coloration with  $\text{Fe}^{2+}$  above 1 ppm, while a P(AAm-co-AMPS)/Bphen gel shows coloration with  $\text{Fe}^{2+}$  above 0.1 ppm [26]. This simple sensor is able to measure iron at the higher limit in drinking water accepted by either the U.S. Environmental Protection Agency (EPA: 0.3 ppm) [85] or the European Environment Agency (EEA: 0.2 ppm) [86]. Using transmission spectrophotometry, even 0.01 ppm can be detected. The sensor is also able to detect iron in more complex matrixes, such as milk or wine, without interference from particles or macromolecules [26]. Even if other ions could be absorbed inside the hydrogel and could complex with BPhen, either no visible color is formed or the intensity is too low to interfere with the color due to the  $(\text{Bphen})_3\text{Fe}^{2+}$  complex. Since some gels (e.g., PNIPAM) can be swollen in nonaqueous solvents, active dyes can be used in nonaqueous media. In that way, acidity could be determined by a dye loaded in the gel in methanol [30]. Moreover, an indicator almost insoluble in water (e.g., bathocuproine) can be loaded in the gel from nonaqueous solvents and be used to detect ions (e.g.,  $\text{Cu}^+$ ) in water. Since hydrogels can be used as solid state electrolytes, iron can be determined as a  $\text{FePhen}$  complex by electrochemical means using a large-area carbon electrode (made by carbonization of a mat of electrospun polymer nanofibers) [47]. In electrochemical sensors with a redox catalyst



inside the gel, if the redox catalyst and the analyte have the same charge, one of them would be excluded from a compact polyelectrolyte. As discussed above, we found that co-ions are not excluded from charged hydrogels; therefore, a redox catalyst (e.g., FePhen) could be loaded inside a charged hydrogel together with an analyte (e.g., nitrite) of opposite charge [24]. Obviously, if the redox catalyst is itself a different phase, the hydrogel could be designed to extract the analyte from the sample. This approach, using a redox oxide (cobalt oxide) to modify the surface of the electrode in contact with the gel, was used. The sensor was able to determine arsenic in drinking water [31], by the preconcentration of the arsenic anions in the cationic gel (P(AMPTAC)). The measurement of the effect of pressure on the resistance in nanocomposites and s-IPNs [16] allows building sensors of pressure and/or touching, which are increasingly used in consumer electronics. While PANI is strongly colored and could not be used in touchscreens, it can be replaced by more transparent conducting polymers, such as PEDOT. Using a better electronic conductor (e.g., reduced graphene oxide) allows for making a nanocomposite with measurable conductivity and good transparency.

### 3.3.4. Biological Systems

#### 3D Cell Scaffolds

Being highly wet solid frameworks, polyacrylamide gels resemble strongly different biological scaffolds (e.g., connective tissue) and could mimic them for the growth and differentiation of biological cells. However, due to the size of typical eukaryotic cells, only gels with large pores (>50 nm dia.) can act as 3D scaffolds for cell growth. PNIPAM-based hydrogels can support bovine fibroblast cell attachment and proliferation for extended periods of time (up to 20 days) without any significant cytotoxic effect [20]. Indeed, PNIPAM hydrogels allows the growth of different cell lines: murine preadipose cells (3T3-L1), human embryonic kidney cells (HEK293), and human carcinoma-derived cells (A549) [38].

#### Immobilization of Bioactive Agents

Nanoporous hydrogels could be used to encapsulate/immobilize bioactive molecules (e.g., enzymes) or microorganisms (e.g., yeast). The gel allows the exchange of reactants and products, while the bioactive agent is isolated from proteolytic enzymes or other agents (e.g., viruses), which could degrade their activity. Bioethanol is usually produced by hydrolysis of starches to sugars, followed by the fermentation of the sugars to ethanol. The hydrolysis is catalyzed by amylases and the fermentation by yeast (e.g., *Saccharomyces cerevisiae*). The enzymes are isolated from fungi and are an expensive input of the process. We immobilize amylases inside a nanocomposite of graphene oxide with a hydrogel matrix [37]. The immobilization of alpha-amylase in a PAAm gel with GO offers several advantages—enhanced retention and better mechanical properties—and allows catalyst reusability. AMY@PAAm-GO shows the same activity from the first to the fifth cycle, contrary to the enzyme immobilized in alginate that shows a sharply decreasing activity during cycles of use.

#### Cell Adhesion Surfaces

Cell adhesion on hydrogel surfaces is modulated by the hydrophilic properties of the polymer matrix and the presence of cell binding molecules. Semi-interpenetration of hyaluronic acid in polyacrylamide hydrogels promotes cell adhesion of live spermatozooids while releasing dead ones. In that way, improvements in bovine sperm quality can be obtained [46]. Moreover, selection of bull sperm cells can be achieved [48].

#### Carriers for Active Principles

Several bioactive principles (enzymes, antibodies, hormones) are labile to conditions in the digestive tract. Therefore, it cannot be administered orally. Encapsulating such substances in hydrogels could allow taking them orally. However, at some point, the protecting hydrogel should swell or degrade to release the active molecules. pH-sensitive hydrogels

do not swell in acid media (since the -COOH groups are neutral) but swell strongly in basic media (where -COO<sup>-</sup> is compensated by mobile ions). Therefore, the carried molecules will be protected in the stomach (acid media) and released in the intestine (basic media). First, a composite of chitosan-decorated CNT with a P(AAm-co-AA) hydrogel matrix loads a larger amount of IgY than the simple hydrogel [17]. IgY maintained only 14% of its biological activity in gastric pH, while IgY protected by the nanocomposite retained up to 85% of its activity [18]. Therefore, there is an in vivo protective efficacy of the nanocomposite matrix for IgY when it is used against enterotoxigenic *Escherichia coli* (ETEC) in piglets. The results showed that treatment of infected piglets with protected IgY reduced significantly the severity of diarrhea [21].

#### Antimicrobial Gels

Hospital bacterial infections proliferate due to bacteria's ability to adhere to and colonize the surfaces of medical devices (as well as implants or wounds) by the formation of bacterial biofilms. Conventional therapy uses broad-spectrum biomolecular antibiotics. However, their widespread use could induce the ecological selection of antibiotic-resistant bacterial strains. One alternative is to cover surfaces or devices with antibacterial films, which do not use bio-based antibiotics. Silver nanoparticles are known to have broad-spectrum antibacterial activity [87]. However, they can also produce ROS and cause damage to normal tissue [88]. Therefore, nanocomposites where Ag nanoparticles are trapped inside nanoporous hydrogel matrixes and only Ag<sup>+</sup> ions leave the matrix could be used as safe antibacterial materials. The nanocomposites made of silver nanoparticles (Ag-NPs) in PNIPAM-based matrixes are obtained by in situ application of UV light to hydrogels loaded with Ag<sup>+</sup> without any additives. These materials show antibacterial activity against *Pseudomonas aeruginosa* by the release of Ag<sup>+</sup> ions, while the Ag-NPs remain inside the matrix. A larger effect is observed when PNIPAM-co-2% AMPS and PNIPAM-co-6%APTMAC are the matrixes of the nanocomposites, since they release Ag<sup>+</sup> ions faster than the PNIPAM matrix [29]. The bacterial death rate using the nanocomposites is higher than when PNIPAM and nanoparticles in solution are used and seem to be related to the large amount of AgNPs contained inside the gels. Inhibition and diffusion (bactericidal and bacteriostatic) effect halos are observed upon the exposure of bacterial cultures. The nanocomposites with higher antibacterial capacity have a PNIPAM-co-6%APTMAC matrix. The materials have the capacity to maintain an aseptic/antiseptic zone for up to 15 days [36].

#### 4. Conclusions

Along this article, the possibility of tuning the properties (swelling degree and rate in water and nonaqueous solvents, mechanical, electrochemical, thermosensitivity, pH sensitivity, mass transport, partition of solutes, hydrophilicity, wetting/adhesion) of gel composites by changing the chemical composition of the polymer chains and composing with other materials is shown. Moreover, the materials can be made in different sizes/forms (nanoporous, macroporous (closed, open), thin films, nano- and microparticles) even as macromolecules with a combination of properties (e.g., block copolymers). Such different forms share common properties but allow new technological applications since a colloidal dispersion (made of nano- or microparticles) could be used as a solution, with a fast response. A thin film has characteristic mass transport time orders of magnitude lower than bulk pieces. In fact, the common properties allow studying behavior with macroscopic samples, which are easy to handle and measure and extrapolate the observed properties to the micro-/nanoscale while detecting emerging properties. At the same time, the study of the actual materials allows for challenging (or confirming) implicit or explicit paradigms in the field. The copolymerization of AAm or PNIPAM with functionalized acrylamides (e.g., AMPS) has shown to be a powerful tool to tune the properties of the gels: LCST [20], swelling degree [20], hydrophilicity [11], cell adhesion [27], and solute partition [13]. The effect of charged groups (e.g., -SO<sub>3</sub><sup>-</sup> from AMPS) on hydrophilicity is stronger than that of groups with hydrogen bonding (e.g., -OH from HMA). Therefore, 2% of AMPS in the

copolymer produces the same effect as 8% of HMA [20]. A similar difference is observed in the swelling degree. However, we found that the swelling of charged gels is significantly lower in cell-growing media (containing nutritive salts) than in pure water [20]. It seems that the ionic force of the solution affects strongly the swelling. While it was shown that the relative monomer reactivities of different acrylamides are similar, the incorporation of large functional groups (e.g., Phen) can make the reactivities different. In those cases, the comonomer ratio in the gel will be different from the feed ratio of the comonomers. Moreover, since conversion degrees are close to 100%, a composition shift will be observed, rendering nonhomogeneous materials. Such behavior renders mechanically weak materials, and the conditions of polymerization/gelation has to be adjusted (e.g., increasing the total monomer concentration) to produce mechanically stable gels [26]. On the other hand, it is possible to combine conducting polymers (CP (e.g., PANI)) with thermosensitive polymers (TSP (e.g., PNIPAM)) in different forms (nanocomposites, semi-interpenetrated networks) and by different ways (in situ formation of CP inside the gel, in situ polymerization of the vinyl monomer around CP nanoparticles, adsorption of nanoparticles inside macroporous gels, adsorption of linear polymers on CP nanoparticles, and even block copolymerization of CP and TSP monomers). In that sense, the accepted paradigm that in situ formation (by CP monomer in situ polymerization) of a CP inside the gel renders a semi-interpenetrated network (s-IPN) was shown to be incorrect since the formation of a nanocomposite, where CP nanoparticles fill up the pores, was observed [19]. The difference with the formation of an s-IPN (or a IPN) by in situ gelation of one vinyl monomer (e.g., acrylamide) inside a preformed gel (e.g., PNIPAM) is that CP is insoluble in the aqueous media, while the polyacrylamides are soluble and grow in solution. However, if the inserted material is insoluble (while the precursor is soluble), the pores are filled with the newly formed material, even if they are made of polymer chains. A further proof of this model was the formation of true s-IPN of PANI [19]. Some properties (e.g., LCST) are different in the nanocomposite and the s-IPN, suggesting that polymer chains of CP and TSP are in close contact in the s-IPN, while separate domains are present in the nanocomposite. To produce the true s-IPN, a PNIPAM gel was swollen in a true solution of PANI in NMP. While it is known that PANI (emeraldine base form) is soluble in NMP, there were little data on the swelling of hydrogel materials in nonaqueous solvents. It was found that PNIPAM swells in polar solvents (e.g., chloroform) but do not swell in non polar solvents (e.g., cyclohexane). Such behavior allows using cyclohexane to only fill the macropores and to determine the macroporosity. On the other hand, it was found that PNIPAM swells significantly (>2000%) in ternary solutions (e.g., water/ethanol/toluene) containing nonswelling solvents (toluene). Since solvation is a local phenomenon, it is possible to swell PNIPAM gels in solutions of molecules only slightly soluble in water (e.g.,  $\beta$ -carotene, 0.55  $\mu$ M [89]) but soluble in toluene, loading them into the gel. Then, evaporating the solvents produces dry hydrogels loaded with the molecule. By re-wetting the hydrogel in water, the poorly soluble molecules are exposed to water as free molecules, ensuring fast dissolution. [30] Local release of slightly soluble drugs from gels allows for reaching bioactive concentrations only in the target organ. The swelling of amphiphilic gels in nonaqueous solvents is a powerful method to increase the loading of the drug, inside the gel, available for release. The same principle could be used to load larger amounts of organic hydrophobic complexing agents (e.g., Bphen) inside gels to create colorimetric [26], or electrochemical [23], sensors. In the latter case, the paradigm of membrane equilibrium (Donnan equilibrium) implies that charged gels (e.g., PAMPS with  $-\text{SO}_3^-$ ) should retain counterions (e.g.,  $\text{Na}^+$ ) and exclude co-ions (e.g.,  $\text{Cl}^-$ ). We used such behavior to preconcentrate arsenic anions inside PAMPTAC gels to detect them in tap water [31]. On the other hand, we found that hydrogels do not behave as simple Donnan cells with a clear solid/solution interphase. The pore structure of the gel contains a significant amount of solution, which could contain co-ions. Moreover, the hydrophobic nature of some gel polymer chains (e.g., PNIPAM) interacts with organic ions (e.g., Rubipy) or drugs (propranolol), inducing positive partition coefficients of the species into the gel [15]. Not only some properties (mechanical, swelling, hydrophilicity) of the materials can be changed

by mixing/compositing, but also new properties (electronic conductivity, absorption of electromagnetic radiation) can be added. Moreover, a “product” (the absence of a property in one of the components nullifies the whole nanocomposite’s property) property is generated, which is a photothermomechanical (since the volume changes induce chemical effects that could be also photothermomechanical) behavior. That is, the absorption of electromagnetic radiation heats up the CP, which drives the LCST transition of the TSP. Similar macroscopic devices could be made by coupling a conductor coil generator with an electromagnet (or piezoelectric) actuator. However, such systems are difficult to make at the micro- and nanoscale. On the other hand, both the electronic conduction (and its associated electronic transition driven by light) in CP and the LCST are molecular phenomena that occur in macroscopic samples but also on samples of micro-, nano-, and macromolecular sizes. Accordingly, the photothermomechanical behavior of a PANI couple with PNIPAM was observed in systems with macro- [13], micro- [42], nano- [49], and macromolecular [39] sizes. Another interesting point is the physical nature of hydrogel/solution interfaces. The standard view describes the interface as one of a solid with a liquid. However, we found that gel microparticles, self-assembled on a charged surface, coalesce into larger microparticles in a liquidlike behavior. Moreover, we found that it is possible to transfer electrons from a rigid conductor (which has roughness features in the micrometer range), in contact with a gel, to ions dissolved in the gel. The electron transfer constant correlates well with the microviscosity of the gel, indicating that no interlayer of solution is present, and the gel decorates the rigid solid in a liquidlike fashion [24].

## 5. Future Studies and Endeavors

Based on the results discussed above, future lines of work could be envisaged, which extend the procedures described (e.g., synthesis of s-IPN) to other cases, try to elucidate if the new phenomena (e.g., swelling in water and nonaqueous solvent) exist in other materials (other than PNIPAM), and explore related behavior, such as UCST transitions. Moreover, relevant factors for technological use, such as durability, stability, and environmental impact, are discussed.

It would be interesting to produce true s-IPN of other conducting polymers with thermosensitive polyacrylamides. However, unmodified polypyrrole or polythiophene does not have known solvents. Alkyl-substituted pyrroles [90] polymerize to render conducting polymers soluble in PC and ACN. Substituted poly(thiophenes) are soluble in organic solvents (e.g., chloroform [91]) and even water [92]. Therefore, s-IPNs could be produced by swelling PNIPAM in CP solutions. Moreover, unlike PANI in NMP, the polymerization renders the soluble form. Therefore, in situ polymerization inside the swollen gel could also render a true s-IPN. Interestingly, the same process could be made by copolymerization of substituted aniline (e.g., orthanilic acid with aniline [93]) to produce PANI in water inside a swollen gel. Both methods could be used to produce s-IPN of CPs (including PANI) soluble in water not only inside PNIPAM but also on other polyacrylamides (e.g., PAAm).

The previously shown results indicate that PNIPAM is an amphiphilic gel, which swells in both water and nonaqueous (even low polarity) solvents [30] and opens a completely new field for both gels and nanocomposites with a gel matrix. It is likely that similar polymers (e.g., PNNDMA) would also show amphiphilic properties. However, we found that other polymers (PAMPTAC and PAAm) swell in water but not in other solvents such as NMP. While this makes them not useful for making true s-IPNs, it would be interesting to produce organized structures using block copolymers (e.g., P(AAm-co-NIPAM), which form gel-like micelle structures. Research has to be made to understand the underlying relationship between polymer structure and swelling, screening homopolymers and copolymers for their swelling properties. It is known that copolymers made of charged monomers bearing the hydrophobic pair (e.g., TAA<sup>+</sup>/TPB<sup>-</sup>) and long alkyl chain acrylates act as ionic polyelectrolytes in nonpolar media (e.g., THF) [94]. Those results suggest that AMPTAC does not swell in NMP because the chloride counterion interacts

only weakly with the solvent. Using a large anion (e.g., perchlorate) or a hydrophobic one (e.g., TPB<sup>−</sup>) could increase the swelling degree. Such ionic gel polyelectrolytes could be of use in leakproof ion-lithium batteries [95]. Useful information to that goal would come out from current work in our laboratory where the swelling capacity of PNIPAM is studied in solvents bearing other functional groups (amines, esters/lactones, heterocycles, anhydrides, polyols), as well as ionic liquids, deep eutectics, and green solvents (e.g., 2-MeTHF). The use of green solvents is a precondition for biological applications. Additionally, we have already observed clear effects of the length of the alkyl chain of the solvents on the swelling degree of PNIPAM [30]. Therefore, different solvents of families bearing the same functional group (e.g., carboxylic acid) will be studied. In hydrogels, it is known that the adsorption of surfactants on the polymer chains affects the swelling degree and LCST of gels in water [96]. It is likely that molecules with a functional group that could interact strongly with polyacrylamides (e.g., alcohols) and tails (e.g., long alkyl chains) that interact with a nonpolar solvent (e.g., cyclohexane) could increase the swelling of amphiphilic gels in those solvents. Besides the academic interest, such swelling of nonpolar liquids could be used to remediate oil spills [97], with low-cost homopolymers. The amphiphilic behavior of the materials is relevant to the use since a dry macroporous gel could be applied to the oil/water mixture and the gel pore surfaces, which adsorb oil, and become exposed by the swelling in the water of the matrix. Until now, the amphiphilic swelling of PNIPAM is studied with macroscopic samples. Since the driving force is molecular, it could work in other size ranges (micro, nano) or shapes (thin film, macroporous gels). It was observed that the swelling rate is inversely proportional to the solvent viscosity [33]. Since several nonaqueous solvents (e.g., eutectic solvents) have large viscosities, the shorter diffusion path-length in small systems (e.g., nanogels) could compensate such effect. Moreover, all those structures have larger surface/volumes ratio than macroscopic samples. Therefore, the intake of the low-polarity organic substance (e.g., a VOC) from solution will be faster due to the large interface area and the short internal path length.

Since the paradigm is that hydrogels are aqueous sponges, we have studied aqueous ion reactions, such as complexation [26], redox catalysis [23], or electrochemical coupled chemical reactions [24], inside the gel. However, organic reactions useful in analytical chemistry [98] or irreversibly binding contaminants [99] could occur inside amphiphilic gels. The reactant could be preloaded from an organic solvent, where it is soluble. Then, the organic solvent is removed, and the gel swollen in aqueous solution of the target chemical. The product of the reaction will remain retained by hydrophobic interactions. However, the gel could be cleaned by swelling in an organic solvent where the product is soluble. If the organic solvent is immiscible with water, it could be left inside the gel. The solute partition between immiscible solvents is usually larger than that between the gel and the solution; therefore, more substance will be reacted. By retaining the solvent (immiscible with water), the interphase is small (external area of the gel). A likely solution involves using other structures (macroporous gels, micro-/nanoparticles) with a larger surface/volume ratio.

The feasibility of performing localized electrochemistry in the region of the gel close to an electrode [23] allows driving electrochemically organic reactions between the preloaded reactant and the absorbed substance [100]. Such method can be used for analytical purposes or to write on the gel surface.

On the other hand, physical changes could alter the materials. We observed that nanoporous films show the formation of breaks/holes when subjected to a vacuum (as required to measure SEM micrographs). It seems that residual water evaporates into bubbles, which create cavities in the soft material. Moreover, superabsorbent films, which include charged monomer units (e.g., AMPS), swell beyond the fracture point of the gels, and the monoliths disintegrate. One way to prevent that involves incorporating another polymer network, making double-network hydrogels [101].

The swelling/deswelling cycles induced by either removing/adding the solvent or heating/cooling the gels through the LCST transition should cause fatigue. However, it has been reported that several cycles do not affect the gels [102]. We have subjected gels to drying/swelling and heating/cycling for more than 50 cycles without changes. In the same way, compression of the gels several times does not induce irreversible deformations.

One relevant point for technological applications involves the durability and stability of this type of materials. In chemical terms, we found that polyacrylamides are highly stable, sustaining heating for 48 h in 6 N HCl (a typical procedure to hydrolyze amides [103]). The mechanical properties are not significantly altered. Some hydrolysis of the amide group is observed, but the cross-links, which in the materials discussed here are made of bis-acrylamide (linked by an amide group), seem to be intact. Such behavior is valuable for permanent devices but make them an ecological hazard. Using biomass-originated hydrogel chemistry (e.g., HPC) allows us to reduce the CO<sub>2</sub> footprint of the materials and make them biodegradable. Moreover, the gels are thermosensitive since HPC shows an LCST in pure water at ca. 42 °C [104]. However, polyacrylamide gels are open networks where the cross-links are made of transversal chains growing from the cross-linker. On the other hand, soluble biopolymers (e.g., CMC) can be cross-linked by the reaction of pending groups (-OH) with bifunctional reactants (e.g., glyoxal) [105]. The resulting gels show low swelling since the cross-links are short. To make more open gels, branched polysaccharides (e.g., amylopectin [106]) could be cross-linked molecularly and chemically modified to link thermosensitive groups [107]. We observed that PNIPAM can absorb large amounts of water and also low-molecular-weight solvents. This amphiphilic behavior can be used for loading significant amounts of hydrophobic drugs to be released in aqueous biological media. However, we tested solvents too toxic to be used in pharmaceutical applications (e.g., chloroform). Therefore, the absorption/swelling of green solvents [108], such as 2-MeTHF, in PNIPAM should be studied.

## 6. Patents

Cesar. A. BARBERO, María A. MOLINA, Claudia R. RIVAROLA, Maria Alicia BIASUTTI, Proceso para la fabricacion de superficies estructuradas y termosensibles usando fotopolimerizacion con luz visible y su correspondiente método para formar imágenes de películas poliméricas, INPI-ARG P 2009 010 4252, 04/11/2009. Granted.

César A. BARBERO, María A. MOLINA, Claudia R. RIVAROLA, *Actuador mecanico y quimico impulsado a distancia usando microondas*, INPI-ARG No. P090100738. 2/03/2009. Requested.

**Author Contributions:** Conceptualization, C.A.B.; data curation, M.V.M., C.R.R., M.A.M. and D.F.A.; writing—original draft preparation, C.R.R., D.F.A. and M.A.M.; writing—review and editing, C.A.B.; supervision, C.A.B. All authors have read and agreed to the published version of the manuscript.

**Funding:** This research was funded by: FONCYT (PICT 2450/2019, PME 2005) CONICET (PIP 1013-2015), SECYT-UNRC (PPI 2001-2003), FAN (Nanopymes), J.S. Guggenheim Foundation (LA-2007), and IRSES-UE (SUMA2).

**Institutional Review Board Statement:** Not applicable.

**Informed Consent Statement:** Not applicable.

**Data Availability Statement:** Not applicable.

**Acknowledgments:** The authors thank the reviewers for their helpful comments and suggestions.

**Conflicts of Interest:** The authors declare no conflict of interest.

## Glossary of Abbreviations

2-MeTHF	2-methyltetrahydrofuran
4-ATF	4-aminothiophenol
AA	acrylic acid
AAM	acrylamide
ACN	acetonitrile
AMPS	2-acrylamido-2-methylpropanesulfonic acid
AMY	$\alpha$ -amylase
AMY@PAAm-GO	$\alpha$ -amylose in PAAm-GO
ANI	aniline
APTMAC	(3-acrylamidopropyl)trimethylammonium chloride
BPhen	bathophenanthroline
CP	conducting polymer
DAMAC	diallyldimethylammonium chloride
DLIP	direct laser interference patterning
DLS	dynamic light scattering
DMF	dimethylformamide
GO	graphene oxide
HBT	human body temperature
HEA	N-hydroxyethylacrylamide
HMA	N-acryloyl-tris-(hydroxymethyl)aminomethane
HPC	hydroxypropylcellulose
IgY	egg yolk immunoglobulin
LCST	lower critical solution temperature
MMA	methylmethacrylate
MTT	3-(4,5-dimethylthiazol-2-yl)-2,5-diphenyltetrazolium bromide
MWNTs	multiwall carbon nanotubes
NAT	N-[Tris(hydroxymethyl)methyl]acrylamide
NIPAM	N-isopropylacrylamide
NIR	near infrared
NMP	N-methylpyrrolidone
PAAm	polyacrylamide
PANI	polyaniline
Pc	partition coefficient
PC	propylene carbonate
PEDOT	poly(ethylenedioxythiophene)
Phen	phenanthroline
PMMA	poly(methylmethacrylate)
PNMANI	poly(N-methylaniline)
PNNDMA	poly(N,N-dimethylacrylamide)
PPy	polypyrrole
rGO	reduced graphene oxide
Rubipy	$\text{Ru}(\text{bipyridine})_3^{2+}$
SDS	sodium dodecyl sulfate
SEM	scanning electron microscopy
s-IPN	semi-interpenetrating network
SPAN 80	sorbitan monooleate
TAA <sup>+</sup>	tetraalkylammonium ion
TEMED	N,N,N',N'-tetramethylethylenediamine
TPB <sup>-</sup>	tetraphenylborate
VOC	volatile organic contaminant

## Appendix A

**Table A1.** Molar fractions of solvents: water, ethanol, and toluene used to make the ternary mixtures tested to swell PNIPAM (Figure 4B).

Mixture	$x_{\text{water}}$	$x_{\text{EtOH}}$	$x_{\text{toluene}}$
M1	0.6341	0.3539	0.01
M2	0.446	0.504	0.05
M3	0.3375	0.5625	0.1
M4	0.2603	0.5397	0.2
M5	0.1048	0.3952	0.5
M7	0.0404	0.2696	0.7

## References

- Yang, T.-H. Recent Applications of Polyacrylamide as Biomaterials. *Recent Pat. Mater. Sci.* **2008**, *1*, 29–40. [CrossRef]
- Osada, Y.; Khokhlov, A. *Polymer Gels and Networks*; CRC Press: Boca Raton, FL, USA, 2001.
- Available online: <https://polymer.bocsci.com/products/acrylamide> (accessed on 7 March 2022).
- Kabiri, K.; Omidian, H.; Zohuriaan-Mehr, M.J.; Doroudiani, S. Superabsorbent hydrogel composites and nanocomposites: A review. *Polym. Compos.* **2011**, *32*, 277–289. [CrossRef]
- Darnell, M.C.; Sun, J.-Y.; Mehta, M.; Johnson, C.; Arany, P.R.; Suo, Z.; Mooney, D.J. Performance and Biocompatibility of Extremely Tough Alginate/Polyacrylamide Hydrogels. *Biomaterials* **2013**, *34*, 8042–8048. [CrossRef] [PubMed]
- Baumann, G.; Chrambach, A. A highly crosslinked, transparent polyacrylamide gel with improved mechanical stability for use in isoelectric focusing and isotachopheresis. *Anal. Biochem.* **1976**, *70*, 32–38. [CrossRef]
- Tang, L.; Wang, L.; Yang, X.; Feng, Y.; Li, Y.; Feng, W. Poly(N-isopropylacrylamide)-based smart hydrogels: Design, properties and applications. *Prog. Mater. Sci.* **2021**, *115*, 100702. [CrossRef]
- Brannon-Peppas, L.; Peppas, N.A. Equilibrium swelling behavior of pH-sensitive hydrogels. *Chem. Eng. Sci.* **1991**, *46*, 715–722. [CrossRef]
- Xiang, T.; Lu, T.; Zhao, W.-F.; Zhao, C.-S. Ionic-Strength Responsive Zwitterionic Copolymer Hydrogels with Tunable Swelling and Adsorption Behaviors. *Langmuir* **2019**, *35*, 1146–1155. [CrossRef]
- Rivarola, C.R.; Biasutti, M.A.; Barbero, C.A. A visible light photoinitiator system to produce acrylamide based smart hydrogels: Ru(bpy)<sub>3</sub><sup>2+</sup> as photopolymerization initiator and molecular probe of hydrogel microenvironments. *Polymer* **2009**, *50*, 3145–3152. [CrossRef]
- Molina, M.A.; Rivarola, C.R.; Barbero, C.A. Evidence of hydrophobic interactions controlling mobile ions release from smart hydrogels. *Mol. Cryst. Liq. Cryst.* **2010**, *521*, 265–271. [CrossRef]
- Molina, M.A.; Rivarola, C.R.; Miras, M.C.; Lescano, D.; Barbero, C.A. Nanocomposite synthesis by absorption of nanoparticles into macroporous hydrogels. Building a chemomechanical actuator driven by electromagnetic radiation. *Nanotechnology* **2011**, *22*, 245504. [CrossRef]
- Molina, M.A.; Rivarola, C.R.; Barbero, C.A. Effect of copolymerization and semi-interpenetration with conducting polyanilines on the physicochemical properties of poly(N-isopropylacrylamide) based thermosensitive hydrogels. *Eur. Polym. J.* **2011**, *47*, 1977–1984. [CrossRef]
- Molina, M.A.; Rivarola, C.R.; Broglia, M.F.; Acevedo, D.F.; Barbero, C.A. Smart surfaces: Reversible switching of a polymeric hydrogel topography. *Soft Matter* **2012**, *8*, 307–310. [CrossRef]
- Molina, M.A.; Rivarola, C.R.; Barbero, C.A. Study on partition and release of molecules in superabsorbent thermosensitive nanocomposites. *Polymer* **2012**, *53*, 445–453. [CrossRef]
- Rivero, R.E.; Molina, M.A.; Rivarola, C.R.; Barbero, C.A. Pressure and microwave sensors/actuators based on smart hydrogel/conductive polymer nanocomposite. *Sens. Actuators B Chem.* **2014**, *190*, 270–278. [CrossRef]
- Bellingeri, R.; Alustiza, F.; Picco, N.; Acevedo, D.; Molina, M.A.; Rivero, R.; Grosso, C.; Motta, C.; Barbero, C.; Vivas, A. In vitro toxicity evaluation of hydrogel-carbon nanotubes composites on intestinal cells. *J. Appl. Polym. Sci.* **2015**, *132*, 41370. [CrossRef]
- Bellingeri, R.V.; Picco, N.Y.; Alustiza, F.E.; Canova, J.V.; Molina, M.A.; Acevedo, D.F.; Barbero, C.; Vivas, A.B. pH-responsive hydrogels to protect IgY from gastric conditions: In vitro evaluation. *J. Food Sci. Technol.* **2015**, *52*, 3117–3122. [CrossRef]
- Martínez, M.V.; Abel, S.B.; Rivero, R.; Miras, M.C.; Rivarola, C.R.; Barbero, C.A. Polymeric nanocomposites made of a conductive polymer and a thermosensitive hydrogel: Strong effect of the preparation procedure on the properties. *Polymer* **2015**, *78*, 94–103. [CrossRef]
- Rivero, R.E.; Alustiza, F.; Rodríguez, N.; Bosch, P.; Miras, M.C.; Rivarola, C.R.; Barbero, C.A. Effect of functional groups on physicochemical and mechanical behavior of biocompatible macroporous hydrogels. *React. Funct. Polym.* **2015**, *97*, 77–85. [CrossRef]



21. Alustiza, F.; Bellingeri, R.; Picco, N.; Motta, C.; Grosso, M.C.; Barbero, C.A.; Acevedo, D.F.; Vivas, A. IgY against enterotoxigenic *Escherichia coli* administered by hydrogel-carbon nanotubes composites to prevent neonatal diarrhoea in experimentally challenged piglets. *Vaccine* **2016**, *34*, 3291–3297. [[CrossRef](#)]
22. Mulko, L.; Rivarola, C.R.; Barbero, C.A.; Acevedo, D.F. Bioethanol production by reusable *Saccharomyces cerevisiae* immobilized in a macroporous monolithic hydrogel matrices. *J. Biotechnol.* **2016**, *233*, 56–65. [[CrossRef](#)]
23. Martínez, M.V.; Rodríguez, R.C.; Moncada, A.B.; Rivarola, C.R.; Bruno, M.M.; Miras, M.C.; Barbero, C.A. Electrochemistry of Tris(1,10-phenanthroline) iron (II) inside a polymeric hydrogel. Coupled chemical reactions and migration effects. *J. Solid State Chem.* **2016**, *20*, 2951–2960. [[CrossRef](#)]
24. Martínez, M.V.; Bruno, M.M.; Miras, M.C.; Barbero, C.A. Electroactive polymers made by loading redox ions inside crosslinked polymeric hydrogels. Effects of hydrophobic interactions and solvent dynamics. *Electrochim. Acta* **2016**, *219*, 363–376. [[CrossRef](#)]
25. Mulko, L.; Yslas, E.; Abel, S.B.; Rivarola, C.; Barbero, C.; Acevedo, D. Smart hydrogels: Application in bioethanol production. In *Handbook of Composites from Renewable Materials*; Thakur, V.K., Thakur, M.K., Kessler, M.R., Eds.; Wiley: New York, NY, USA, 2017; Volume 1, pp. 79–105. [[CrossRef](#)]
26. Martínez, M.V.; Rivarola, C.R.; Miras, M.C.; Barbero, C.A. A colorimetric iron sensor based on the partition of phenanthroline complexes into polymeric hydrogels. Combinatorial synthesis and high throughput screening of the hydrogel matrix. *Sens. Actuators B Chem.* **2017**, *241*, 9–32. [[CrossRef](#)]
27. Rivero, R.; Alustiza, F.; Capella, V.; Liaudat, C.; Rodríguez, N.; Bosch, P.; Barbero, C.; Rivarola, C. Physicochemical properties of ionic and non-ionic biocompatible hydrogels in water and cell culture conditions: Relation with type of morphologies of bovine fetal fibroblasts in contact with the surfaces. *Colloids Surf. B Biointerfaces* **2017**, *158*, 488–497. [[CrossRef](#)]
28. Pereyra, J.Y.; Cuello, E.A.; Rodríguez, R.C.; Barbero, C.A.; Yslas, E.I.; Salavagione, H.J.; Acevedo, D.F. Synthesis and characterization of GO-hydrogels composites. In *IOP Conference Series: Materials Science and Engineering*; IOP Publishing: Bristol, UK, 2017; Volume 258, p. 012002. [[CrossRef](#)]
29. Monerri, M.; Brogna, M.; Yslas, I.; Barbero, C.; Rivarola, C. Antibacterial polymeric nanocomposites synthesized by in-situ photoreduction of silver ions without additives inside biocompatible hydrogel matrices based on N-isopropylacrylamide and derivatives. *Express Polym. Lett.* **2017**, *11*, 946–962. [[CrossRef](#)]
30. Martínez, M.V.; Molina, M.A.; Abel, S.B.; Barbero, C.A. Large Swelling Capacities of Crosslinked Poly(N-isopropylacrylamide) Gels in Organic Solvents. *MRS Adv.* **2018**, *3*, 3735–3740. [[CrossRef](#)]
31. Martínez, M.V.; Rodríguez, R.C.; Bruno, M.M.; Acevedo, D.F.; Barbero, C.A. Simple electrochemical detection method employing a hydrogel soft matrix: Application in tap water. *J. Electrochem. Soc.* **2018**, *165*, H1021–H1027. [[CrossRef](#)]
32. Bellingeri, R.; Mulko, L.; Molina, M.; Picco, N.; Alustiza, F.; Grosso, C.; Vivas, A.; Acevedo, D.F.; Barbero, C.A. Nanocomposites based on pH-sensitive hydrogels and chitosan decorated carbon nanotubes with antibacterial properties. *Mater. Sci. Eng. C* **2018**, *90*, 461–467. [[CrossRef](#)] [[PubMed](#)]
33. Martínez, M.V.; Molina, M.; Barbero, C.A. Poly(N-isopropylacrylamide) Cross-Linked Gels as Intrinsic Amphiphilic Materials: Swelling Properties Used to Build Novel Interphases. *J. Phys. Chem. B* **2018**, *122*, 9038–9048. [[CrossRef](#)] [[PubMed](#)]
34. Brogna, M.F.; Balmaceda, I.; Carrizo, F.; Barbero, C.A.; Rivarola, C.R. Acid hydrogel matrixes as reducing/stabilizing agent for the in-situ synthesis of Ag-nanocomposites by UV irradiation: pH effect. *Mater. Res. Express* **2019**, *6*, 055021. [[CrossRef](#)]
35. Pereyra, J.; Martínez, M.V.; Barbero, C.; Bruno, M.; Acevedo, D. Hydrogel-graphene oxide nanocomposites as electrochemical platform to simultaneously determine dopamine in presence of ascorbic acid using an unmodified glassy carbon electrode. *J. Compos. Sci.* **2019**, *3*, 1. [[CrossRef](#)]
36. Monerri, M.; Brogna, M.F.; Yslas, E.I.; Barbero, C.A.; Rivarola, C.R. Highly effective antimicrobial nanocomposites based on hydrogel matrix and silver nanoparticles: Long-lasting bactericidal and bacteriostatic effects. *Soft Matter* **2019**, *15*, 8059–8066. [[CrossRef](#)]
37. Mulko, L.; Pereyra, J.Y.; Rivarola, C.R.; Barbero, C.A.; Acevedo, D.F. Improving the retention and reusability of Alpha-amylase by immobilization in nanoporous polyacrylamide-graphene oxide nanocomposites. *Int. J. Biol. Macromol.* **2019**, *122*, 1253–1261. [[CrossRef](#)]
38. Capella, V.; Rivero, R.E.; Liaudat, A.C.; Ibarra, L.E.; Roma, D.A.; Alustiza, F.; Mañas, F.; Barbero, C.A.; Bosch, P.; Rivarola, C.R.; et al. Cytotoxicity and bioadhesive properties of poly-N-isopropylacrylamide hydrogel. *Heliyon* **2019**, *5*, e01474. [[CrossRef](#)]
39. Abel, S.B.; Riberi, K.; Rivarola, C.R.; Molina, M.; Barbero, C.A. Synthesis of a smart conductive block copolymer responsive to heat and near infrared light. *Polymers* **2019**, *11*, 1744. [[CrossRef](#)]
40. Rivero, R.E.; Capella, V.; Liaudat, A.C.; Bosch, P.; Barbero, C.A.; Rodríguez, N.; Rivarola, C.R. Mechanical and physicochemical behavior of a 3D hydrogel scaffold during cell growth and proliferation. *RSC Adv.* **2020**, *10*, 5827–5837. [[CrossRef](#)]
41. Riberi, K.; Abel, S.B.; Martínez, M.V.; Molina, M.A.; Rivarola, C.R.; Acevedo, D.F.; Rivero, R.; Cuello, E.A.; Gramaglia, R.; Barbero, C.A. Smart thermomechanochemical composite materials driven by different forms of electromagnetic radiation. *J. Compos. Sci.* **2020**, *4*, 3. [[CrossRef](#)]
42. Abel, S.B.; Rivarola, C.R.; Barbero, C.A.; Molina, M. Electromagnetic radiation driving of volume changes in nanocomposites made of a thermosensitive hydrogel polymerized around conducting polymer nanoparticles. *RSC Adv.* **2020**, *10*, 9155–9164. [[CrossRef](#)]
43. Mulko, L.E.; Cuello, E.A.; Barbero, C.A.; Pino, G.A.; Molina, M.; Rossa, M. Remote radiofrequency triggering of topography changes in a surface micropatterned PANI@PNIPAM nanocomposite. *Appl. Surf. Sci.* **2020**, *509*, 145370. [[CrossRef](#)]

44. Casadey, R.; Broglia, M.; Barbero, C.; Criado, S.; Rivarola, C. Controlled release systems of natural phenolic antioxidants encapsulated inside biocompatible hydrogels. *React. Funct. Polym.* **2020**, *156*, 104729. [[CrossRef](#)]
45. Abel, S.B.; Molina, M.; Rivarola, C.R.; Barbero, C.A. Pickering emulsions stabilized with PANI-NP. Study of the thermoresponsive behavior under heating and radiofrequency irradiation. *J. Appl. Polym. Sci.* **2021**, *138*, 50625. [[CrossRef](#)]
46. Blois, D.A.; Liaudat, A.C.; Capella, V.; Morilla, G.; Rivero, R.E.; Broglia, M.F.; Barbero, C.A.; Rodríguez, N.; Bosch, P.; Rivarola, C.R. Interaction between Hyaluronic Acid Semi-Interpenetrated Hydrogel with Bull Spermatozoa: Studies of Sperm Attachment–Release and Sperm Quality. *Adv. Mater. Interfaces* **2021**, *8*, 2101155. [[CrossRef](#)]
47. Bongiovanni Abel, S.; Martínez, M.V.; Bruno, M.M.; Barbero, C.A.; Abraham, G.A.; Acevedo, D.F. A modular platform based on electrospun carbon nanofibers and poly(N-isopropylacrylamide) hydrogel for sensor applications. *Polym. Adv. Technol.* **2021**, *32*, 4815–4825. [[CrossRef](#)]
48. Liaudat, A.C.; Blois, D.; Capella, V.; Morilla, G.; Rivero, R.; Barbero, C.; Rodríguez, N.; Rivarola, C.; Bosch, P. Bull sperm selection by attachment to hyaluronic acid semi-interpenetrated hydrogels. *Reprod. Domest. Anim.* **2022**, *57*, 228–232. [[CrossRef](#)] [[PubMed](#)]
49. Abel, S.B.; Molina, M.A.; Rivarola, C.R.; Kogan, M.J.; Barbero, C.A. Smart polyaniline nanoparticles with thermal and photothermal sensitivity. *Nanotechnology* **2014**, *25*, 495602. [[CrossRef](#)]
50. Cavallo, P.C.; Muñoz, D.J.; Miras, M.C.; Barbero, C.; Acevedo, D.F. Extracting kinetic parameters of aniline polymerization from thermal data of a batch reactor. Simulation of the thermal behavior of a reactor. *J. Appl. Polym. Sci.* **2014**, *131*, 39409. [[CrossRef](#)]
51. Klomsiri, C.; Karplus, P.A.; Poole, L.B. Cysteine-based redox switches in enzymes. *Antioxid. Redox Signal.* **2011**, *15*, 1065–1077. [[CrossRef](#)] [[PubMed](#)]
52. Henríquez, I.C.; Bueno, C.; Lissi, E.A.; Encinas, M.V. Thiols as chain transfer agents in free radical polymerization in aqueous solution. *Polymer* **2003**, *44*, 5559–5561. [[CrossRef](#)]
53. Panda, P.K.; Dash, P.; Biswal, A.K.; Chang, Y.-H.; Misra, P.K.; Yang, J.-M. Synthesis and Characterization of Modified Poly (vinyl alcohol) Membrane and Study of Its Enhanced Water-Induced Shape-Memory Behavior. *J. Polym. Environ.* **2022**, *30*, 3409–3419. [[CrossRef](#)]
54. Panda, P.K.; Yang, J.-M.; Chang, Y.-H. Water-induced shape memory behavior of poly (vinyl alcohol) and p-coumaric acid-modified water-soluble chitosan blended membrane. *Carbohydr. Polym.* **2021**, *257*, 117633. [[CrossRef](#)]
55. Cuello, E.A.; Mulko, L.E.; Barbero, C.A.; Acevedo, D.F.; Yslas, E.I. Development of micropatterning polyimide films for enhanced antifouling and antibacterial properties. *Colloids Surf. B Biointerfaces* **2020**, *188*, 110801. [[CrossRef](#)]
56. Stockert, J.C.; Horobin, R.W.; Colombo, L.L.; Blázquez-Castro, A. Tetrazolium salts and formazan products in Cell Biology: Viability assessment, fluorescence imaging, and labeling perspectives. *Acta Histochem.* **2018**, *120*, 159–167. [[CrossRef](#)]
57. Zhang, Z.; Tang, L.; Chen, C.; Yu, H.; Bai, H.; Wang, L.; Qin, M.; Feng, Y.; Feng, W. Liquid metal-created macroporous composite hydrogels with self-healing ability and multiple sensations as artificial flexible sensors. *J. Mater. Chem. A* **2021**, *9*, 875–883. [[CrossRef](#)]
58. Acevedo, D.F.; Martínez, G.; Arana, J.T.; Yslas, E.I.; Mucklich, F.; Barbero, C.; Salavagione, H.J. Easy way to fabricate nanostructures on a reactive polymer surface. *J. Phys. Chem. B* **2009**, *113*, 14661–14666. [[CrossRef](#)]
59. Molina, M.; Asadian-Birjand, M.; Balach, J.; Bergueiro, J.; Miceli, E.; Calderón, M. Stimuli-responsive nanogel composites and their application in nanomedicine. *Chem. Soc. Rev.* **2015**, *44*, 6161–6186. [[CrossRef](#)]
60. Molina, M.A. Development of Nano-Composites Based on Smart Hydrogels and Nano-Objects. Ph.D. Thesis, National University of Rio Cuarto, Rio Cuarto, Argentina, 1 May 2007.
61. Martínez, M.V. Development of Polymeric Nanomaterials with Specific Solute Retention. Ph.D. Thesis, National University of Rio Cuarto, Rio Cuarto, Argentina, 23 July 2015.
62. Balach, J.; Bruno, M.M.; Cotella, N.G.; Acevedo, D.F.; Barbero, C.A. Electrostatic self-assembly of hierarchical porous carbon microparticles. *J. Power Source* **2012**, *199*, 386–394. [[CrossRef](#)]
63. Decher, G.; Eckle, M.; Schmitt, J.; Struth, B. Layer-by-layer assembled multicomposite films. *Curr. Opin. Colloid Interface Sci.* **1998**, *3*, 32–39. [[CrossRef](#)]
64. Fan, L.; Ge, X.; Qian, Y.; Wei, M.; Zhang, Z.; Yuan, W.-E.; Ouyang, Y. Advances in Synthesis and Applications of Self-Healing Hydrogels. *Front. Bioeng. Biotechnol.* **2020**, *8*, 654. [[CrossRef](#)]
65. Pollack, G.H. *Cells, Gels and the Engines of Life*; Ebner and Sons Publishers: New York, NY, USA, 2001.
66. Caykara, T.; Bulut, M.; Dilsiz, N.; Akyüz, Y. Macroporous poly(acrylamide) hydrogels: Swelling and shrinking behaviors. *J. Macromol. Sci. A* **2006**, *43*, 889–897. [[CrossRef](#)]
67. Da Silva, L.B.J.; Oréfice, R.L. Synthesis and electromechanical actuation of a temperature, pH, and electrically responsive hydrogel. *J. Polym. Res.* **2014**, *21*, 466. [[CrossRef](#)]
68. Torres, M.L.; Oberti, T.G.; Fernández, J.M. HEMA and alginate-based chondrogenic semi-interpenetrated hydrogels: Synthesis and biological characterization. *J. Biomater. Sci. Polym. Ed.* **2021**, *32*, 504–523. [[CrossRef](#)]
69. Zhao, S.; Wang, Z.; Wang, J.; Yang, S.; Wang, S. PSf/PANI nanocomposite membrane prepared by in situ blending of PSf and PANI/NMP. *J. Membr. Sci.* **2011**, *376*, 83–95. [[CrossRef](#)]
70. Hüther, A.; Xu, X.; Maurer, G. Swelling of n-isopropyl acrylamide hydrogels in water and aqueous solutions of ethanol and acetone. *Fluid Phase Equilib.* **2004**, *219*, 231–244. [[CrossRef](#)]
71. Orlov, Y.; Xu, X.; Maurer, G. Equilibrium swelling of N-isopropyl acrylamide based ionic hydrogels in aqueous solutions of organic solvents: Comparison of experiment with theory. *Fluid Phase Equilib.* **2006**, *249*, 6–16. [[CrossRef](#)]

72. Orlov, Y.; Xu, X.; Maurer, G. Swelling of nonionic N-isopropyl acrylamide hydrogels in aqueous solutions of (acetic acid or pyridine). *Fluid Phase Equilib.* **2005**, *238*, 87–94. [CrossRef]
73. Althans, D.; Langenbach, K.; Enders, S. Influence of different alcohols on the swelling behaviour of hydrogels. *Mol. Phys.* **2012**, *110*, 1391–1402. [CrossRef]
74. Wu, S.; Shanks, R.A. Solubility study of polyacrylamide in polar solvents. *J. Appl. Polym. Sci.* **2004**, *93*, 1493–1499. [CrossRef]
75. Narváez, W.E.V.; Jiménez, E.L.; Hernández-Rodríguez, M.; Rocha-Rinza, T. Simple method to estimate relative hydrogen bond basicities of amides and imides in chloroform. *J. Mol. Struct.* **2018**, *1173*, 608–611. [CrossRef]
76. Lanzalaco, S.; Armelin, E. Poly(N-isopropylacrylamide) and Copolymers: A Review on Recent Progresses in Biomedical Applications. *Gels* **2017**, *3*, 36. [CrossRef]
77. Din, M.I.; Khalid, R.; Akbar, F.; Ahmad, G.; Najeeb, J.; Hussain, Z.U.N. Recent progress of poly(N-isopropylacrylamide) hybrid hydrogels: Synthesis, fundamentals and applications—Review. *Soft Mater.* **2018**, *16*, 228–247. [CrossRef]
78. Adelson, P.D. Hypothermia following Pediatric Traumatic Brain Injury. *J. Neurotrauma* **2009**, *26*, 429–436. [CrossRef] [PubMed]
79. Planes, G.A.; Miras, M.C.; Barbero, C. Strong effects of counterions on the electrochemistry of poly(N-methylaniline) thin films. *Polym. Int.* **2002**, *51*, 429–433. [CrossRef]
80. Bard, A.J.; Faulkner, L.R. *Electrochemical Methods: Fundamentals and Applications*, 2nd ed.; Wiley: New York, NY, USA, 2000.
81. Lira, L.M.; de Torresi, S.I.C. Conducting polymer–hydrogel composites for electrochemical release devices: Synthesis and characterization of semi-interpenetrating polyaniline–polyacrylamide networks. *Electrochem. Commun.* **2005**, *7*, 717–723. [CrossRef]
82. Marcus, R.A. On the Theory of Electron-Transfer Reaction VI. Unified Treatment of Homogeneous and Electrode Reactions. *J. Chem. Phys.* **1965**, *43*, 679. [CrossRef]
83. Muya, F.N.; Sunday, C.E.; Baker, P.; Iwuoha, E. Environmental remediation of heavy metal ions from aqueous solution through hydrogel adsorption: A critical review. *Water Sci. Technol.* **2016**, *73*, 983–992. [CrossRef]
84. Grygolowicz-Pawlak, E.; Crespo, G.A.; Afshar, M.G.; Mistlberger, G.; Bakker, E. Potentiometric Sensors with Ion-Exchange Donnan Exclusion Membranes. *Anal. Chem.* **2013**, *85*, 6208–6212. [CrossRef]
85. Available online: <http://www.water-eseach.net/index.php/standards/secondary-standards> (accessed on 22 June 2022).
86. Available online: <http://eur-lex.europa.eu/legal-content/EN/TXT/?uri=CELEX:31998L0083> (accessed on 22 June 2022).
87. Bruna, T.; Maldonado-Bravo, F.; Jara, P.; Caro, N. Silver Nanoparticles and Their Antibacterial Applications. *Int. J. Mol. Sci.* **2021**, *22*, 7202. [CrossRef]
88. Chairuangkitti, P.; Lawanprasert, S.; Roytrakul, S.; Aueviriyavit, S.; Phummiratch, D.; Kulthong, K.; Chanvorachote, P.; Maniratanchote, R. Silver nanoparticles induce toxicity in A549 cells via ROS-dependent and ROS-independent pathways. *Toxicol. In Vitro* **2013**, *27*, 330–338. [CrossRef]
89. Share, H.; Ali, M.; Asl, H.; Khajenoori, M. Experimental measurement and correlation of solubility of  $\beta$ -carotene in pure and ethanol-modified subcritical water, Chinese. *J. Chem. Eng.* **2020**, *28*, 2620–2625. [CrossRef]
90. Masuda, H.; Tanaka, S.; Kaeriyama, K. Soluble conducting polypyrrole: Poly(3-octylpyrrole). *J. Chem. Soc. Chem. Commun.* **1989**, *11*, 725–726. [CrossRef]
91. Wang, L.; Wu, X.; Wang, X.; Feng, Q.; Pei, M.; Zhang, G. Synthesis and characterization of three novel conjugated polythiophene derivatives. *Des. Monomers. Polym.* **2013**, *16*, 339–348. [CrossRef]
92. Lanzi, M.; Salatelli, E.; Giorgini, L.; Mucci, A.; Pierini, F.; Di-Nicola, F.P. Water-soluble polythiophenes as efficient charge-transport layers for the improvement of photovoltaic performance in bulk heterojunction polymeric solar cells. *Eur. Polym. J.* **2017**, *97*, 378–388. [CrossRef]
93. Barbero, C.; Kötzt, R. Electrochemical formation of a self-doped conductive polymer in the absence of a supporting electrolyte. The copolymerization of o-aminobenzenesulfonic acid and aniline. *Adv. Mater.* **1994**, *6*, 577–580. [CrossRef]
94. Ono, T.; Ohta, M.; Sada, K. Ionic polymers act as polyelectrolytes in nonpolar media. *ACS Macro Lett.* **2012**, *1*, 1270–1273. [CrossRef]
95. Sun, X.-G.; Liu, G.; Xie, J.; Han, Y.; Kerr, J.B. New gel polyelectrolytes for rechargeable lithium batteries. *Solid State Ion* **2004**, *175*, 713–716. [CrossRef]
96. Caykara, T.; Izol, D.; Birlik, G.; Akaoğlu, B. Adsorption of surfactant by hydrophobically modified Poly [2-(diethylamino) ethylmethacrylate-co-N-vinyl-2-pyrrolidone/octadecyl acrylate] hydrogels and effect of surfactant adsorption on the volume phase transition. *J. Appl. Polym. Sci.* **2007**, *103*, 3771–3775. [CrossRef]
97. Ono, T.; Sada, K. Toward the design of superabsorbent materials for non-polar organic solvents and oils: Ionic content dependent swelling behaviour of cross-linked poly (octadecyl acrylate)-based lipophilic polyelectrolytes. *J. Mater. Chem.* **2012**, *22*, 20962–20967. [CrossRef]
98. Shimamoto, G.G.; Aricetti, J.A.; Tubino, M. A Simple, Fast, and green titrimetric method for the determination of the iodine value of vegetable oils without wajs solution (ICL). *Food Anal. Methods* **2016**, *9*, 2479–2483. [CrossRef]
99. Gesser, H.D.; Fu, S. Removal of Aldehydes and Acidic Pollutants from Indoor Air. *Environ. Sci. Technol.* **1990**, *24*, 495–497. [CrossRef]
100. Ma, Y.; Wu, S.; Jiang, S.; Xiao, F.; Deng, G.-J. Electrosynthesis of azobenzenes directly from nitrobenzenes. *Chin. J. Chem.* **2021**, *39*, 3334–3338. [CrossRef]
101. Zhang, M.; Zhang, D.; Chen, H.; Zhang, Y.; Liu, Y.; Ren, B.; Zheng, J. A multiscale polymerization framework towards network structure and fracture of double-network hydrogels. *Npj Comput. Mater.* **2021**, *7*, 39. [CrossRef]

102. Dharmasiri, M.B.; Mudiyansele, T.K. Thermo-responsive poly (N-isopropyl acrylamide) hydrogel with increased response rate. *Polym. Bull.* **2021**, *78*, 3183–3198. [[CrossRef](#)]
103. Pei, Y.; Zhao, L.; Du, G.; Li, N.; Xu, K.; Yang, H. Investigation of the degradation and stability of acrylamide-based polymers in acid solution: Functional monomer modified polyacrylamide. *Petroleum* **2016**, *2*, 399–407. [[CrossRef](#)]
104. Weißenborn, E.; Braunschweig, B. Hydroxypropyl cellulose as a green polymer for thermo-responsive aqueous foams. *Soft Matter* **2019**, *15*, 2876–2883. [[CrossRef](#)]
105. Abel, S.B. Synergistic Nanocomposites Based on Thermosensitive and Conductive Polymers. Ph.D. Thesis, National University of Rio Cuarto, Rio Cuarto, Argentina, 23 February 2018.
106. Salemis, P.; Rinaudo, M. Molecular weight-viscosity relationship for amylopectin, a highly branched polymer. *Polym. Bull.* **1984**, *12*, 283–285. [[CrossRef](#)]
107. Fu, Z.; Zhang, L.; Ren, M.-H.; BeMiller, J.N. Developments in Hydroxypropylation of Starch: A Review. *Starch* **2019**, *71*, 1800167. [[CrossRef](#)]
108. Pace, V.; Hoyos, P.; Fernández, M.; Sinisterra, J.V.; Alcántara, A.R. 2-Methyltetrahydrofuran as a suitable green solvent for phthalimide functionalization promoted by supported KF. *Green Chem.* **2010**, *12*, 1380–1382. [[CrossRef](#)]